University College of Southeast Norway

www.usn.no

FMH606 Master's Thesis 2017

Industrial It and automation

Modelling and estimation for return mud flow during drilling

Ivan Alejandro Pirir Ruiz

Faculty of Technology, Natural sciences and Maritime Sciences

Campus Porsgrunn

University College of Southeast Norway

www.usn.no

Course: FMH606 Master's Thesis, 2017

Title: Modelling and estimation for return mud flow during drilling

Number of pages: 86

Keywords: Oil drilling, Solid control system, Open channel flow, Flow estimation

Student: Ivan Alejandro Pirir Ruiz

Supervisor: Roshan Sharma

External partner: Statoil, Kelda drilling controls ASA

Availability: Open

Approved for archiving: _____

(supervisor signature)

Summary:

Oil drilling is performed to retrieve gas and petroleum from reservoirs that can be kilometers down the earth surface. During a drilling operation, drilling fluid is pumped into the well to remove cuttings and maintain a stable pressure. A multitude of models that describe the dynamics of the drill fluid through the bottom side of the drilling operation have been developed through the years. However, there is a lack of models that describe the topside flow loop. This is the case since the flow of mud through the return line has traditionally been directly measured using paddle and Coriolis meters.

With an increase in demand of accuracy and an interest to avoid the use of Coriolis meters to reduce costs, the interest in alternative ways to describe the drill fluid circulation through the system has increase. One of which is with the use of mathematical models.

In this project, a model for the drain back to the active pit was developed and tested for various operational scenarios as well as giving description for the different parts of the topside flow loop. In addition to this, model based estimation of flow using a Venturi channel was tested and compared with the traditional method using Bernoulli's equation, as this can be an alternative way to measure the discharge from a return line. The results of the comparison were similar using the experimental data available.

Preface

The following are the result from my master thesis. A complete model for a drilling operation including the top side flow has never been develop to my knowledge. This is not because there has not been a genius as big as me to develop it (especially since the model in reality very simple), but because there was no need for it. The marked has changed and the prices of oil are steadily declining and this will continue in the future. Now is important to optimize the system to reduce prices but keeping the safety of the workers as the highest priority.

I want to thank my supervisor Roshan Sharma for helping me with this project and to my fried Harrison Idornigie for making this past two years ever so slightly less painful.

Porsgrunn, 15.5.2017

Ivan Alejandro Pirir Ruiz

Nomenclature

β_d	Bulk modulus of the fluid at the drill string
β_a	Bulk modulus of the fluid at the annulus
$\bar{\rho}_d$	Average density of the fluid at the drill sting
$\bar{\rho}_a$	Average density of the fluid at the annulus
ρ_{cl}	Density of the drill mud after the solid control system
ρ_{cu}	Density of the dry cuttings
Q_{pump}	Discharge of the mud pump
Q_{bit}	Discharge at the drill bit
Q_{res}	Discharge from the reservoir
Q_{back}	Discharge from the backpressure pump
Q_{pipe}	Discharge at the end of the flowline
Q_{cl}	Discharge of clean mud after the solid control system
Q_{cu}	Discharge of dry cuttings
Q_{loss}	Discharge of losses of clean drill mud from cuttings
V_d	Volume of the drill string
V_a	Volume of the annulus
p_p	Pressure at the mud pump
p_c	Pressure at the choke valve
p_{bit}	Pressure at the drill bit
p_0	Atmospheric pressure
F_a	Friction at the annulus
F_d	Friction at the drill string
S_f	Friction term of a channel
K_c	Valve constant of the choke valve
h_{bit}	Hight of the drill bit
h_T	Fluid level inside the active mud pit
z_c	Opening of the choke valve (%/10)
Ar_{bT}	Base area of the mud pit
φ	Angle between a horizontal line and a channel bed
S_L	Side slope of a channel

S_0	Slope of a channel
w	Width of a channel
W	Width of the base of a channel
P_w	Wetted perimeter
T	Free surface i.e. part of a flow that is expose to the atmospheric pressure
D	Diameter of the cross-sectional area of a circular pipe

Contents

1 Introduction

With the lowering prices of oil, new ways to decrease the cost of drilling without compensating with higher risks for the workers or the environment are of interest. One way is to replace the Coriolis meter use to measure the discharge through the return line. Instead cheaper sensors can be used along with a mathematical model of the system to compensate for the inaccuracies.

This report describes the development of a model for the top side flow loop that is the part of an oil drilling system that consist of the flowline, solid control system, mud pits and mud pumps. To model the flowline, the 1D Saint Venant equations were used and solved using the Kurganov-Petrova second order central upwind scheme (also known as the KP07 scheme). In this report, it is only included the development of the model without validation as there was not experimental data available to do so. The model was then combine with a model for the well and simulated for some relevant operational scenarios.

One cost efficient way to measure the discharge from the flowline is to use a Venturi channel to estimate the flow using level sensors and Bernoulli's equation. A mathematical model of a Venturi channel using the 1D Saint Venant and the KP07 scheme was also developed. It is showed that the model works using only one boundary condition for the cross-sectional area of the flow. This means that the value of only one level sensor is needed to simulate the flow and there is no need for a boundary condition for the discharge. This can be used to estimate the flow by either taking the discharge directly from the results of the simulation or by looking at the changes in the cross-sectional area of the simulated flow.

1.1 Structure of the report

This report can be divided into three sections:

- Part I: Development of the topside flow loop model and simulations of the combine model with both the top and bottom parts of the system. This includes an overview of both sections of the combine model. This conforms chapter 2 to 8.
- Part II: Flow estimation using a Venturi flume. Here a mathematical model of a Venturi flume was develop and use to estimate the flow going through a real Venturi channel. The results were then compared with the traditional method using Bernoulli's equation which is also described on this section. This conforms chapter 9 to 11.
- Part III: Some suggestions for future works and conclusions for the previous two parts. This conforms the last two chapters, chapters 12 and 13.

Part I

Topside flow loop model

2 Overview of an oil drilling operation

Oil drilling is performed by drilling rigs where a drill bit is attached to a large pipe often called drill string. The drill bit is lowered and rotated using a drive system at the top side and used to cut or crush rocks, soil etc. At the same time a fluid normally referred to as “drill mud” is pumped through the drill string into the well. The drill mud will then flow upwards through the annulus (the space between the drill string and the well) and through a valve called choke vale to a return line. It is then filtered to remove the cuttings from the fluid and then re-circulated into the system. Figure 2-1 shows a simplified overview of the drilling fluid circulation.

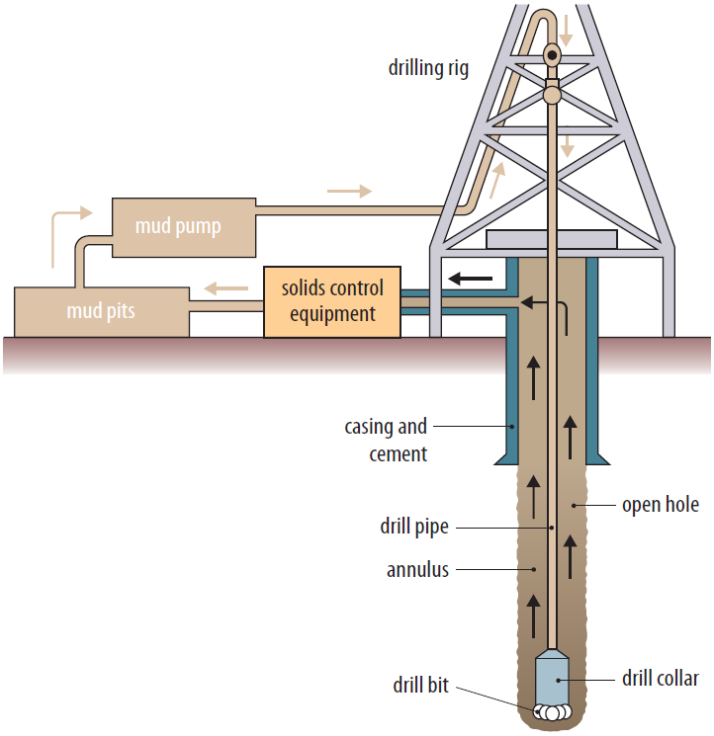

Figure 2-1 Drilling fluid circulating system [1]

The mud circulation has multiple purposes, the two most important being to retrieve the cuttings from the bottom of the well and to control the pressure in the well. This last one will be critical while being near the reservoir (at the reservoir zone). The pressure in the well is kept higher than the reservoir pore pressure. Otherwise it will cause the drilling fluids to penetrate the reservoir formation and results in a loss in the circulated drill mud.

In the other hand if the pressure in the well is lower than the reservoir pore pressure, the reservoir fluids will flow into the annulus which is known as kick. If the occurrence of a kick is nor regulated, it can cause a blowout where the fluids from the reservoir rise uncontrolled to the surface. This can cause massive environmental damages as exemplified by the Deepwater Horizon oil spill that occurred on the 10th of April 2010 where around 4.9 million barrels of oil were spilled into the Gulf of Mexico.

During the drilling operation, different disturbances that will affect the pressure in the well will occur. One will be the change in the hydrostatic pressure of the well cause by the

changes in length of the well, by rising and lowered the drill string (surge and swab) and during tripping. The pore pressure will change as the drill bit gets near the reservoir and so will the flows in or out of the reservoir. Another big disturbance occurs during a pipe connection procedure to extend the length of the drill string. During pipe connections, the mud pump is temporarily stopped to connect a new section of the drill string. If the pressure is not controlled, it can reach dangerously low levels which will result in a blowout.

2.1 Model of the bottom side of a drilling operation

A model was used to study the circulation of drill mud in and out of the well. This model uses two control volumes, one from the drill string and one for the annulus. For a detailed explanation of the model refer to [2].

From the drill string, the pressure at the top will depend on the drilling fluid pumped by the mud pump and the fluid going out of the drill string though a non-return valve installed at the drill bit and into the annulus:

$$\frac{V_d}{\beta_d}\dot{p}_p = Q_{pump} - Q_{bit} \tag{2.1}$$

From the annulus, the pressure at the top will depend on the flow from the drill string, the flow going out of the annulus through the choke valve, the mud pumped by the backpressure pump and flow going into or out of the reservoir. There will also be a change in the volume inside the annulus (depending on the drilling rate):

$$\frac{V_a}{\beta_a}\dot{p}_c = Q_{bit} + Q_{back} - Q_{choke} + Q_{res} - \dot{V}_a \tag{2.2}$$

There are losses due to friction along the system both through the drill string and the annulus:

$$MQ_{bit} = p_p - p_c - F_d|Q_{bit}|Q_{bit} - F_a|Q_{bit} + Q_{res}|(Q_{bit} + Q_{res}) + (\bar{\rho}_d - \bar{\rho}_a)gh_{bit} \tag{2.3}$$

The bottom hole pressure can be calculated as follows:

$$p_{bit} = p_c + M_a Q_{bit} + F_a|Q_{bit} + Q_{res}|(Q_{bit} + Q_{res}) + \bar{\rho}_a g h_{bit} \tag{2.4}$$

The flow through the choke valve that flows from the annulus, can be modelled using a standard valve equation:

$$Q_{choke} = K_c z_c \sqrt{\frac{2}{\bar{\rho}_a}(p_c - p_0)}$$

2.2 Simulation of a drilling operation

To look more into the disturbances that will take place during a drilling operation, two scenarios were simulated. The first one is for a pipe connection procedure, and the second one is to simulate the drilling string going down and up inside the annulus. The model parameter used are described in Table 2-1. These values were taken from [3]. All the simulations were done using MatLab.

Table 2-1 Parameters for the simulation

Parameter	Value	Description
V_d	28.2743	Volume drill string (m^3)
β_d	14000	Bulk modulus drill string (bar)
β_a	14000	Bulk modulus annulus (bar)
K_c	0.0046	Choke valve constant
p_0	1	Atmospheric pressure (bar)
ρ_a	0.0129	Density annulus (10^-5 * kg/m^3)
ρ_d	0.0125	Density drill string (10^-5 * kg/m^3)
F_d	0.165	Friction factor drill string
F_a	0.0208	Friction factor annulus
M_a	1.6009	(10^-8 * kg/m^4)
M_d	5.7296	(10^-8 * kg/m^4)
L_{dN}	3600	Total length drill string (m)
V_a^0	96.1327	Initial volume at the annulus (m^3)
h_{bit}^0	2000	Initial depth of the drill bit (m)
L_{bit}^0	3600	Total length of the well (m)

2.2.1 Pipe connection

For this type of operation, the mud pump needs to stop pumping mud into the annulus. To compensate for this and to avoid the pressure at the well from going below the pore pressure, the choke valve will be closed and mud will be pump into the annulus by using a backpressure pump. The challenge with this type of operation is that during this there will not be any measurements of the pressure at the bottom of the well nor at the return line (in case the choke valve is close entirely). Figure 2-2 shows the results of the simulation. The first plot shows the control inputs, in this case all the control is manual. Here z_c is the opening of the choke valve.

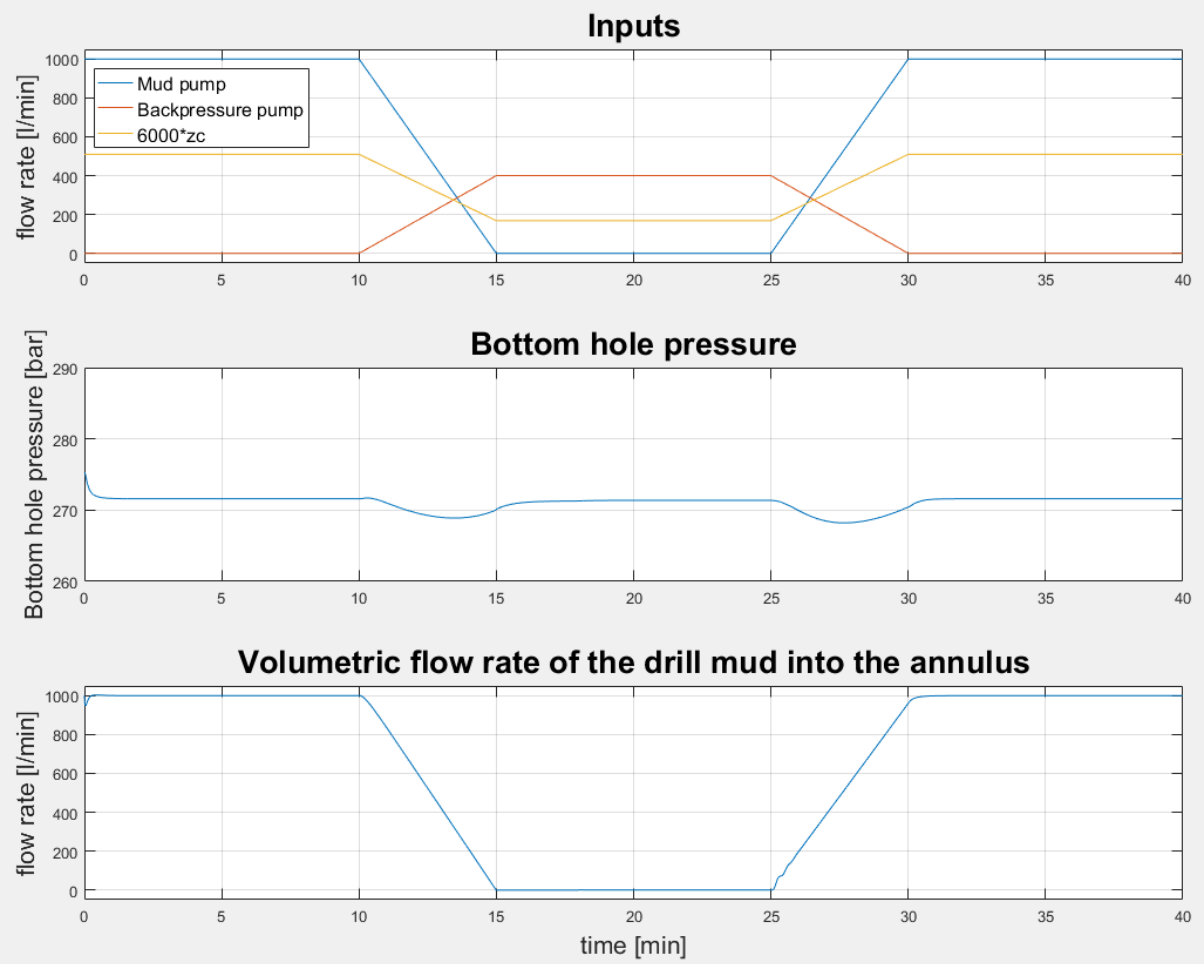

Figure 2-2 Simulations of a pipe connection

2.2.2 Surge and Swab

Moving the drill string into the annulus will cause the drilling fluid to rise, this is called surge. Doing the opposite and pulling the drill string out of the well will temporally decrease the discharge of fluid going out of the well, this is called swabbing. Moving the drill string up and down inside the well, will also cause changes in the pressure inside the well as showed in figure 2-3. This will be specially the case during tripping where the drill string is pulled out of the well and then lowered back which is done to replace the drill bit or in case the drill string is damaged.

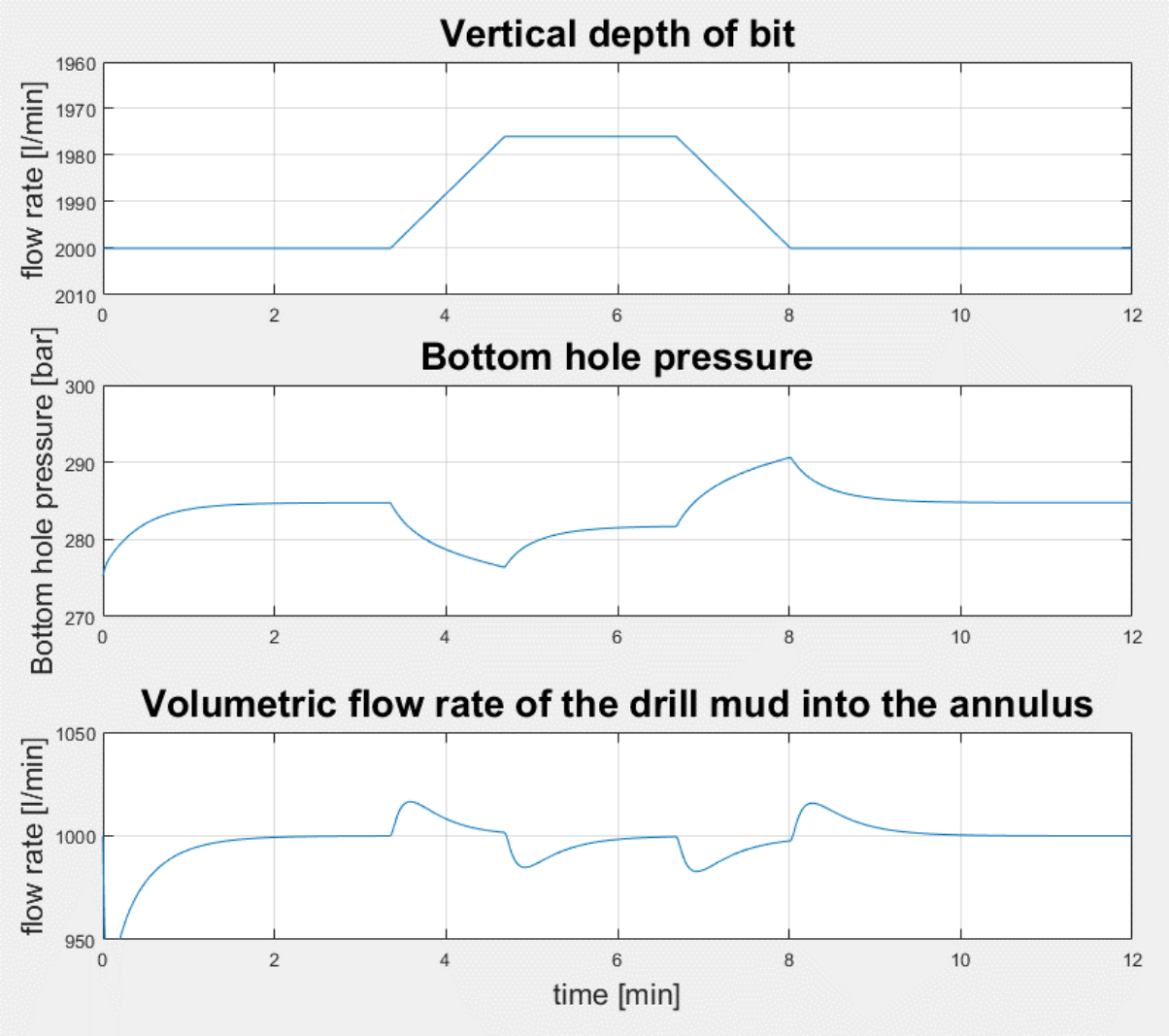

Figure 2-3 Simulation of drill movements

2.3 Kick detection and top side drill flow measurements

The reservoir pore pressure is very difficult to measure. Depending on the location this can be a very uncertain number. This and the fact that controlling the density of the drilling mud is also challenging, signifies the importance of detecting the kick as early as possible. [4]

One indicator of a kick is the sudden increase in drilling rate, however this can vary depending on the drilling bit as different types of drilling bit will increase the penetration rate faster than others. Another indicator is the decrease in pump pressure cause by the reduced hydrostatic weight in the annulus. It can take some time before this change happens so is not regard as a good predictor.

The occurrence of a kick is normally predicted by measuring the flow rate in the return line or by looking at the change in the level of the mud pit. An increase in the flow rate can mean that some of the reservoir fluid have entered the annulus which means that a kick has occurred. In the other hand if the flow decreases, it would mean that some of the drill fluid has flow out of the annulus. The return line is partially filled so only a small set of flowmeters can be used to measure the flow through it. In practice, it is measured using Coriolis mass flowmeters. Other type of flowmeters like paddle flowmeters are still use in older rigs, however they can give very inaccurate measurements. Some rigs use trip tanks to measure the volume of drill mud at the annulus during a pipe connection procedure or during tripping where there will be no mud flowing through the return line or the flow is too small to be measurable. A trip tank is a small tank that is connected to the annulus when the mud pump stops circulation fluid into the well. Drill fluid will circulate in and out of the trip tank depending on the lever of the annulus. By measuring the level in the tank, one can indirectly measure the pressure inside the annulus.

In the case that a kick is detected, oil rigs have a blowout preventer system use to seal the well and inject fluid or gases into the well to stabilize it. However, if the kick is detected too late the system can fail.

In this thesis, the focus is primarily on estimation the flow in the return line, which can be used as a signal for kick/loss detection. In addition, the changes in the active mud pit level will also be considered as an input to the kick/loss detection methods. However, this thesis does not deal with the kick/loss detection methods.

2.4 Simulation of the changes in the flow in and out of the reservoir

It is of interested to study how the occurrence of kick/loss influence the flow in the return line i.e. the return fluid flow. The model use in chapter 2.1 was simulated to test how the outflow from the from the choke valve will change depending on the influx or outflux of fluid from the reservoir. For this simulation, the mud pump was set to be constant equal to 1000 l/min and the opening of the choke valve constant equal to 70%. The only changing value was the flow from the reservoir which was set to 0 l/min initially, and then increased to 200 l/min at 375 seconds (6.25 minutes). Figure 2-4 shows the results of simulated a loss of drill mud from the annulus and figure 2-5 shows the results for an influx of fluid from the reservoir. These figures show how the flow from the choke valve (the flow entering the return line) changes but not abruptly and there will always be delay.

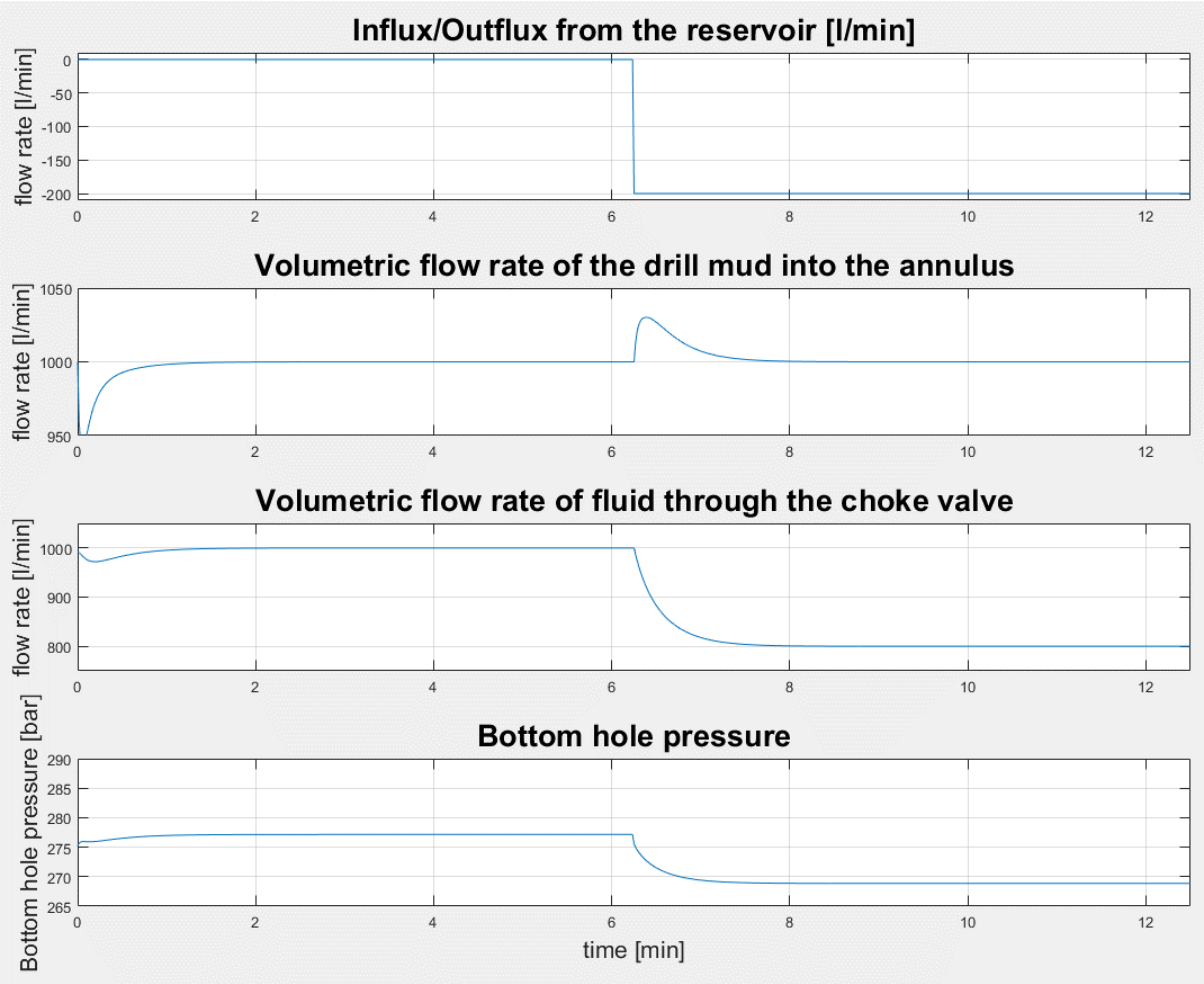

Figure 2-4 Fluid loss from the annulus

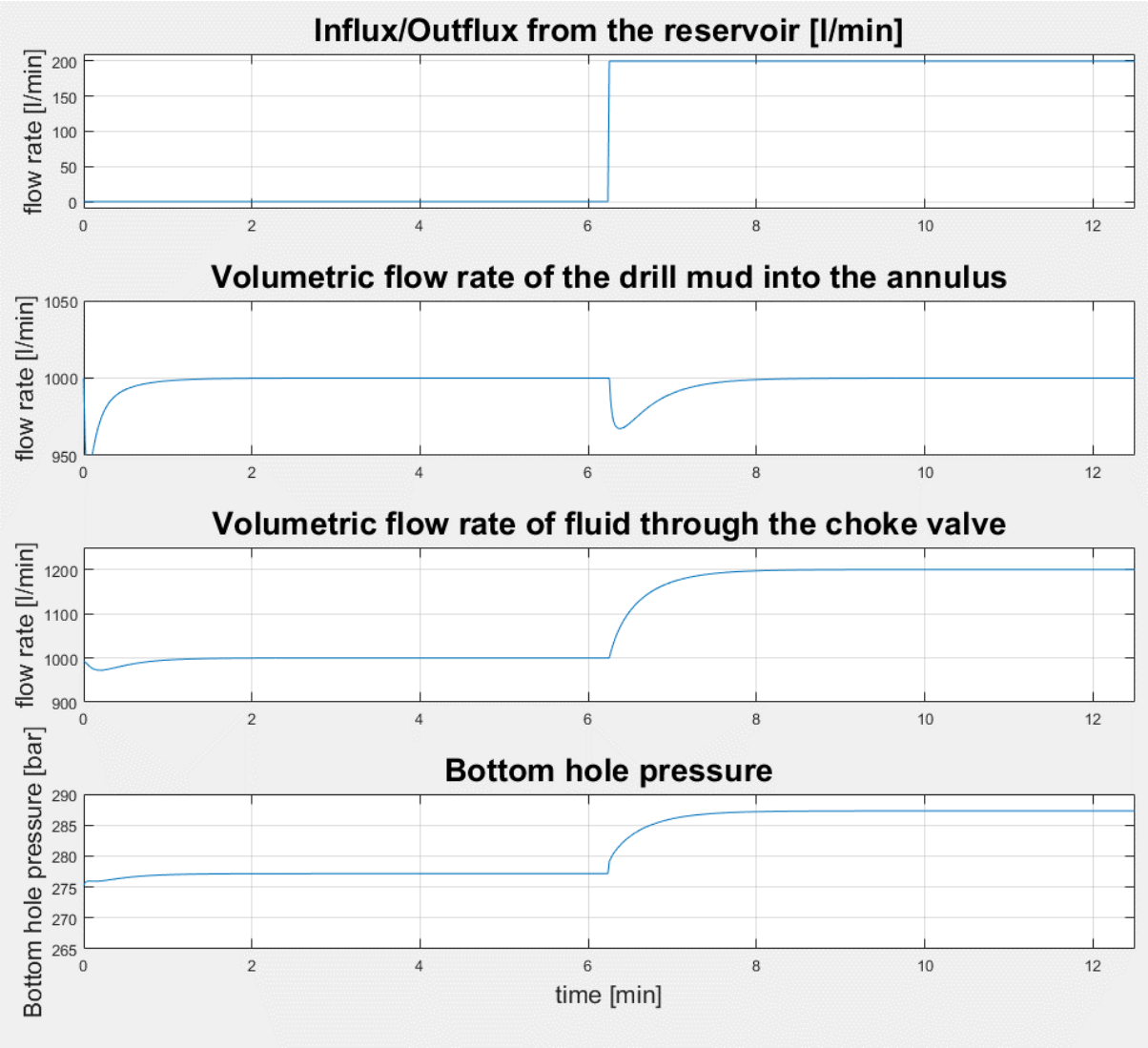

Figure 2-5 Influx from the reservoir

3 Top side flow loop

The top side of a drilling operation consist in a return line also called flowline, an arrangement of devises use to remove the cuttings from the drill fluid (a solid control system) and a set of tanks used to store the drilling fluid called mud pits.

3.1 Solids control system

During a drilling operation, drilling fluid is pumped to the well through the annulus. The drill mud is used to retrieve solids from the bottom of the well to the surface, exert hydrostatic pressure against the walls of the well to prevent fluids from flowing into the well and to cool and lubricate the drilling string and drilling bit. It also should not cause corrosion of the drilling equipment or cause any adverse effects upon the formation being penetrated. [5] [6]

The mud flowing from the annulus carries cuttings (sometimes refer just as solids) out of the well. The presence of solids in drilling fluid will cause an increase in density and viscosity. In the past, these cuttings have been used as a cheap way to increase the weight of the drilling mud. This is no longer a common practice since it has been proved to have many negative effects. Some examples of the adverse effects are: Reduced penetrated rate caused by the formation of mud cakes near the drill bit. Decreased bit life and increased rate of wear pump parts. Greater difficulty in maintaining optimum rheological properties etc. These are some of the reasons why there is a need of a solid control system to clean the drilling mud before it is reused. [7]

The type and the properties of a drill mud is dependent on the wellbore. Some examples are Water-base muds, Oil-base muds and synthetic muds. Water-base muds (also called aqueous drilling fluids) are the most commonly used type of drilling fluid because they are cheaper and easier to clean than other types of muds and are suitable for most operations. These types of fluids will normally contain barite (principally composed of barium sulfate) as a weighting material and bentonite to increase the viscosity. To eliminate the smallest drill cuttings while keeping most of the useful minerals and chemicals is the greatest challenge of a solid control system. Failure to remove drilled solids with solids-control equipment leads to solids control with dilution. Dilution refers to the process of adding a liquid phase (normally more drilling mud) to a drilling fluid to decrease the drilled-solids concentration. This will increase the cost of drilling and is avoided as much as possible. [8]

3.1.1 Overview of the system

The setup of the solid control system changes depending on the type of drill fluid in use and the wellbore. In general, a shale shaker is situated at the beginning of the system and will remove most of the big cuttings. Some setups will also include some type of gumbo removal equipment at the start e. g. scalper shakers or gumbo traps. The smallest cuttings are remove using decanting centrifuges, these devices have also become standard and are present in most newer oil rigs. Other devices like mud cleaners, distillers and desanders are also commonly used to remove the medium-size particles. The drilling fluid from the well will also contain

gas bubbles. To separate the gas from the drilling fluid, a degasser is installer after the main shale shaker.

One common setup for the solid removal system is showed on figure 3-1. Here the term active pit is used to refer to the last partition of the mud pit where the drilling fluid is considered clean and ready to put back into the system. After the shale shaker and between every device, the fluid will be place into different partitions of the mud pit. Some setups will include a desander and a distiller instead of the mud cleaner and other will include a scalper shaker and or a gumbo trap before the shale shaker. Mud cleaners are more commonly use with weighted mud while desanders and distiller are use with unweighted mud. Weighted muds are muds that include some type of additive to increase its density like barite.

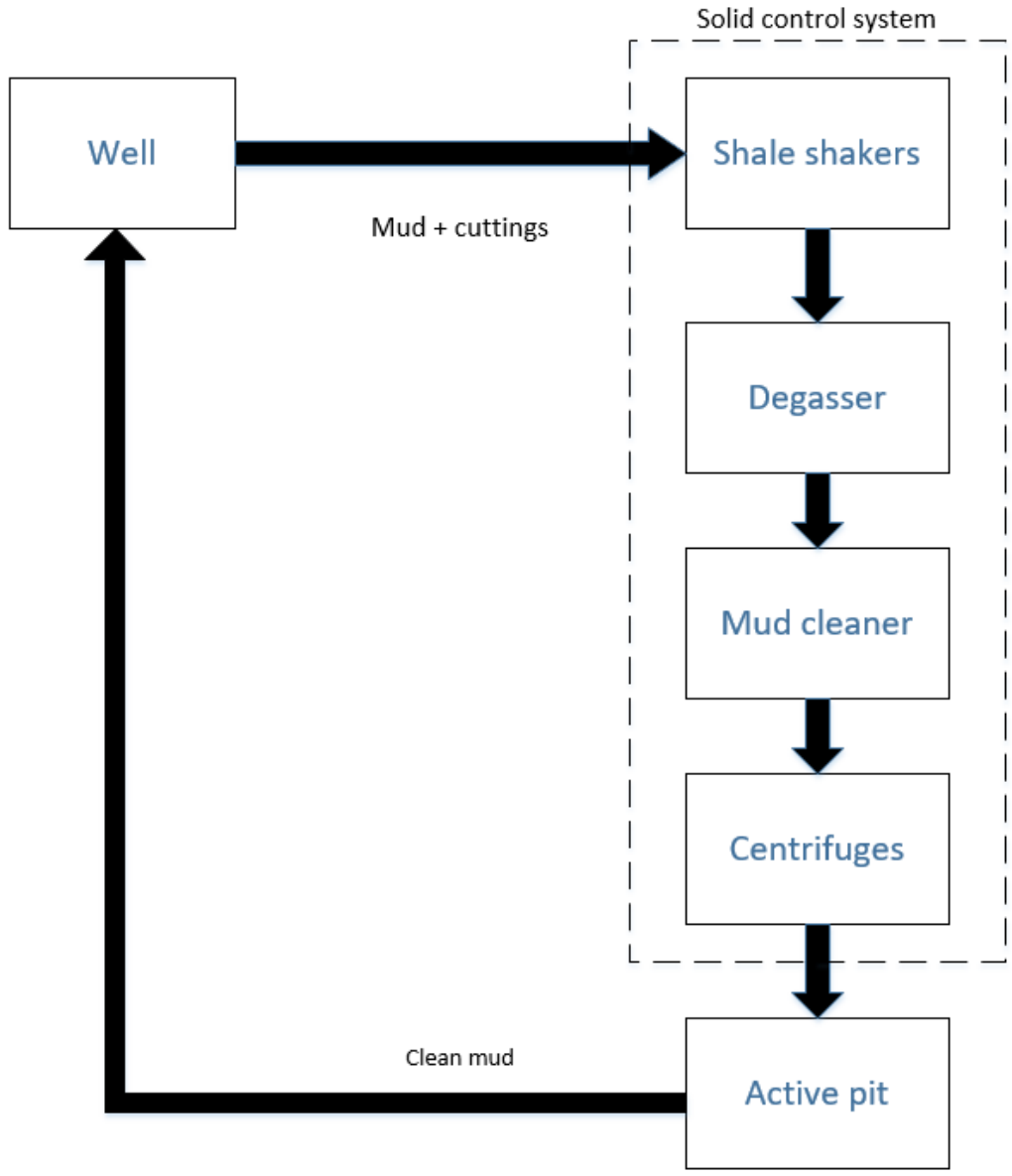

Figure 3-1 A simplified diagram of the top side flow loop

3.1.2 Shale shakers

Shale shakers are the initial and commonly consider the most important drilled-solids removal device. These types of devices impart a vibratory motion to a plastic mesh screen. This motion allows the drilling fluid to pass through the holes of the screen and removes larges particles depending on the size of the openings in the screen. The lower the values of the plastic viscosity and the weight of the drilling fluid, the finer the mesh screen can be used. Common sizes used in the industry for water-base muds range from API 140 to API 200 which is also commonly called 200-mesh. This should not be confused with the previous unofficial measurement that was related to the number of openings per square inch. The official standard by the American Petroleum Institute (API) is related to the size of the openings and the size of the particles that it allows to pass through the screen, and uses microns as the measuring unit. The size API 200 allows particles up to around 74 microns to pass through the screen. This size will allow the baritone and most of the barite particles to flow through the screen while removing most of the big and intermediate size cuttings. [9, 10]

Figure 3-2 shows the working principle of a shale shaker. Most shale shakers use a back tank (called feeding cabin in figure 3-2) to receive the fluid from the flow line. Depending on the model the mud could pass through multiple screens before reaching the exit. Normally multiple shakers are used in parallel to process all the circulating fluid as there is a maximum amount of fluid that each shaker can process without reducing the efficiency.

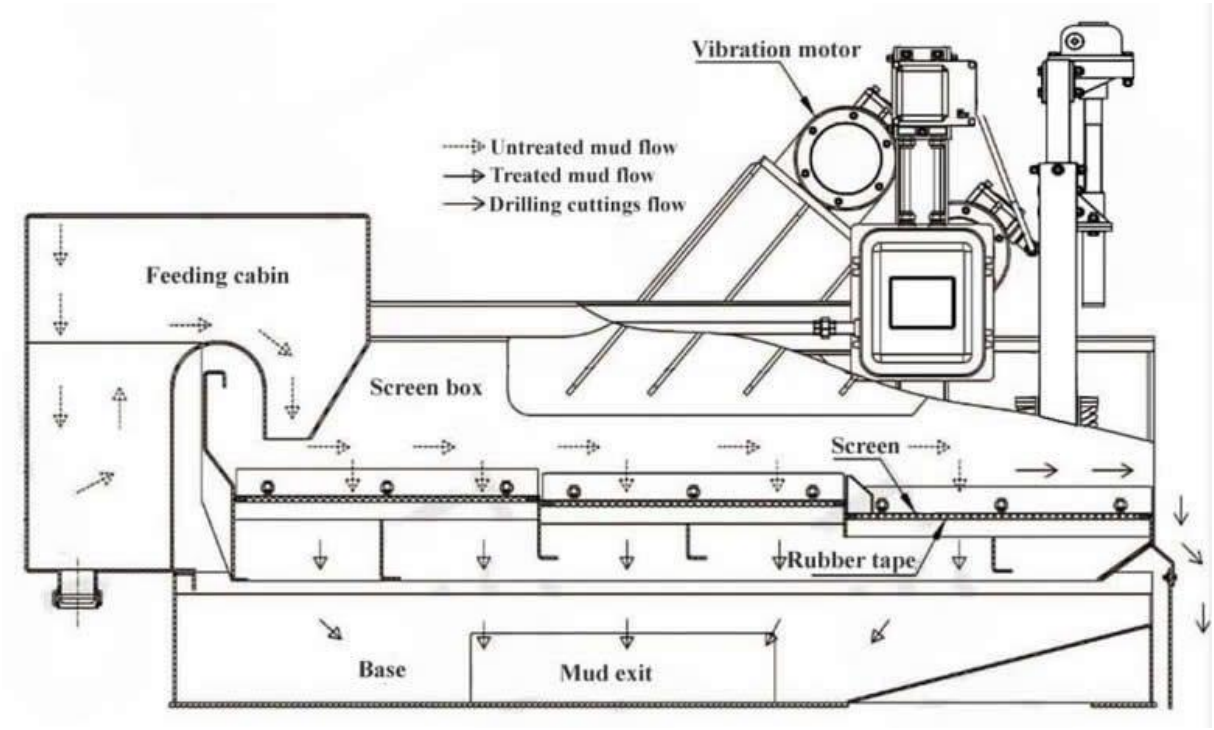

Figure 3-2 Shale shaker working principle [11]

In the cases where there are large quantities of big solid particles or gumbo flowing from the return line, another shale shaker with lager openings should be installed before the main shale shaker. This shaker is often referred to as scalping shaker.

3.1.3 Gumbo removal

Small, sticky drilled solids that hydrate as they move up an annulus, forming large of cuttings are called gumbo. They are formed in the annulus from the adherence of sticky particles to each other. This type of mass is difficult to screen and can affect the efficiency of the main shake shakers so it needs to be remove before it reaches them. Gumbo removal is done by scalper shaker or gumbo traps, this are boxes that contain screens with wide openings. Gumbo is not always prevalent so not all systems need a gumbo removal device. [12]

3.1.4 Hydrocyclones

Hydrocyclones are devises shape like inverted cones with sizes that range from 4 to 12 inches in diameter. These devises separate the heavier materials by adding a spiral motion that propels the drilling fluid. This will cause the heavier particles to move outward against the walls of the cone, the particles will then exit though the bottom while the lighter particles will be forced to the center and exit from the top. The size of the solids discarded depends on the size of the hydrocyclone. The smaller the diameter, the finer are the cuttings discarded. Figure 3-3 shows the working principle of a hydrocyclone.

Hydrocyclones are used in mud cleaners where between six and ten hydrocyclones are arranged. The discarded materials from the cyclones flow into a fine mesh screen. The solids retained by the screen are discarded while the rest goes back to the system. Desanders and distillers also use hydrocyclones of different sizes. [13]

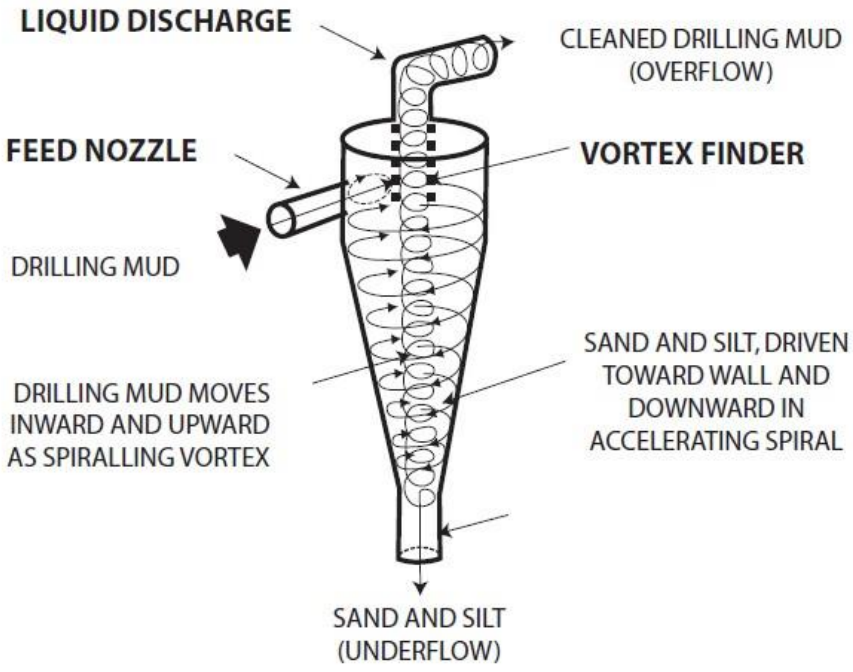

Figure 3-3 Hydrocyclone working principle [14]

3.1.5 Decanting centrifuges

Centrifuges are used to remove very small particles that can be colloidal-sized (less than two microns in size). The presence of these particles can increase the viscosity of the drilling fluid, which will make harder to maintain an optimum level.

The drill mud is fed into the middle of an Archimedes screw that rotates inside a conical tube which also rotates at a higher speed in the same direction. The centripetal forces separate solids from liquids inside the cone. The cuttings are discarded on the narrow side of the centrifuge while the fluid flows to the wider side of the centrifuge and back into the system. Figure 3-4 shows the working principle of a centrifuge. Normally only a fraction of the circulated fluid will be process by the centrifuges, which can be around 25%. The rest of the mud will flow directly to the active mud pit. [15]

Another type of centrifuge called perforated rotor centrifuge is also use in the industry but it is not as common.

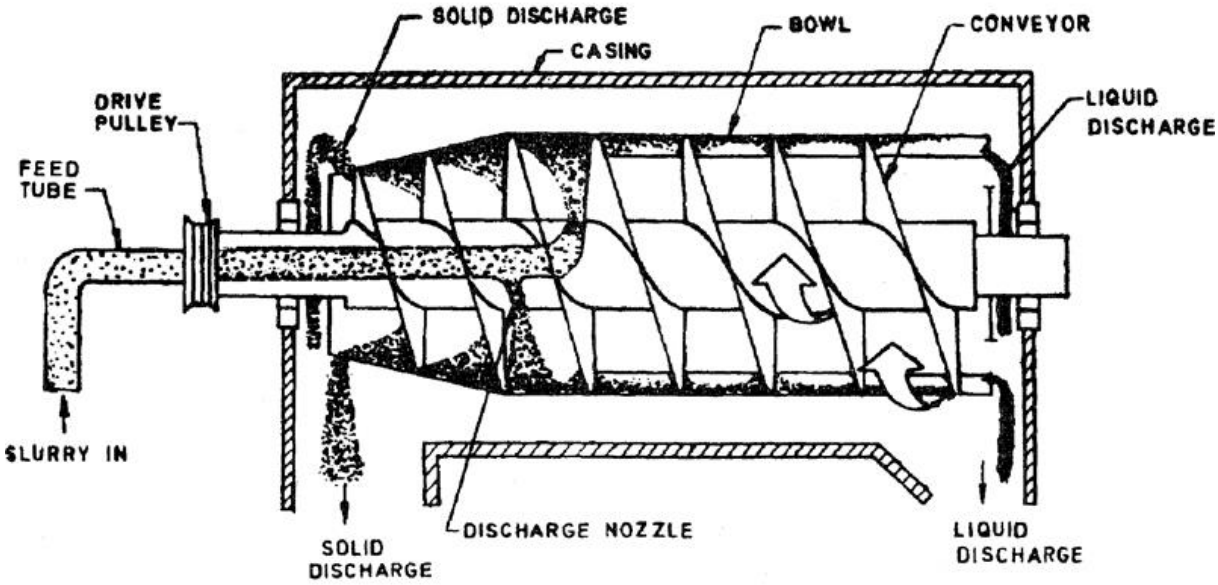

Figure 3-4 Centrifuge working principle [16]

3.1.6 Drying shakers

Dryers are used to minimize the liquid discharge and to make easier to dispose the waste. A drying shaker is a type of shaker with finer screens that the main shale shakers. The discharge from the other solid removal devices flows into the dryer shaker, the liquids that pass through the screens then go back to the system through a decanting centrifuge place to remove the smaller cuttings.

3.2 Mud pits

The drilling fluid is retained at different sections of the solid control system. Most steel pits for drilling fluid are square or rectangular with flat bottoms. Tank agitators, mud guns and/or blenders are used to homogenize the fluid inside the pits. Figure 3-5 shows and example of a mud pit setup. The mud pit is divided in different partitions, each partition will receive the output flow from each section of the solids control system. One can also divide this system into two parts, the removals section and the additions section. [17]

The additions section is where measurements are taken and supplements to increase the density/viscosity are added. If there is any need to add more drill fluid for dilution, this will also be done in this section.

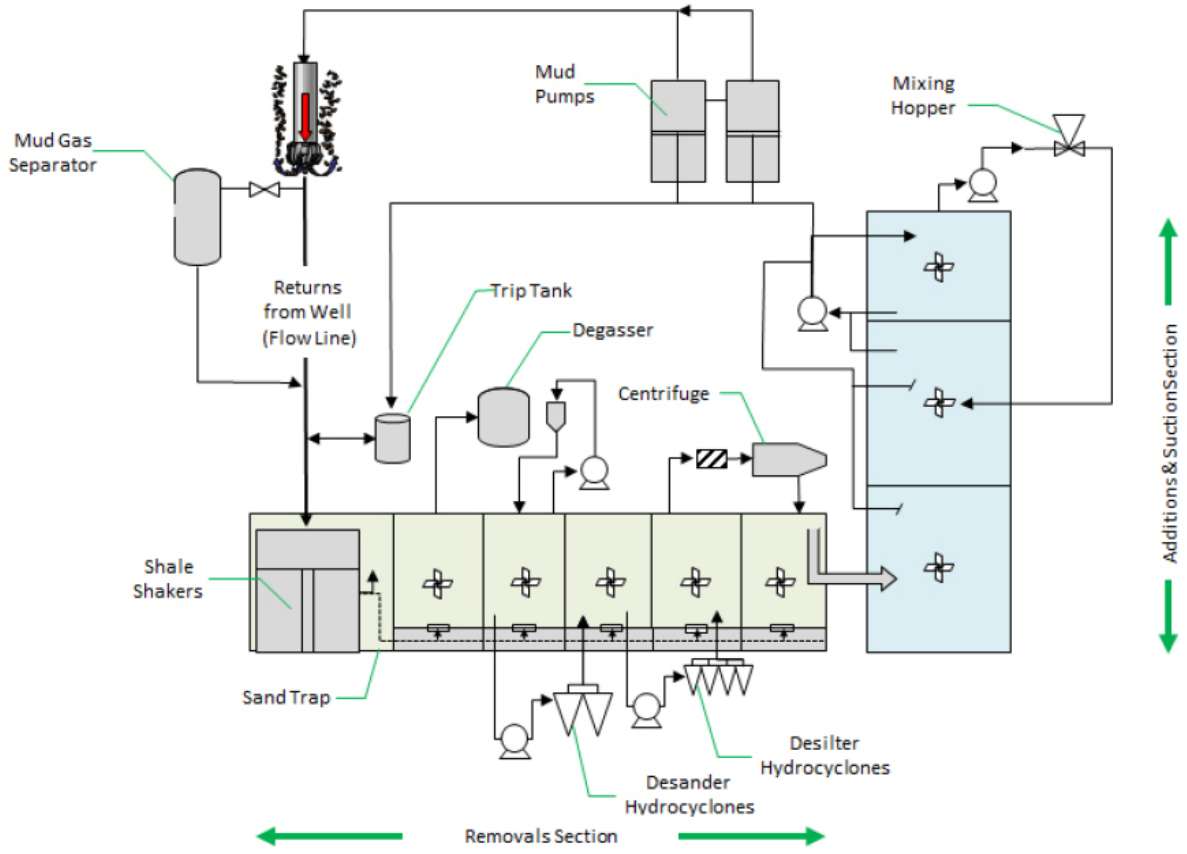

Figure 3-5 An example of a mud pit setup for unweighted mud [18]

3.3 Step by step explanation of the system

This is a description of a common setup for a solid control system + mud pit, however is important to keep in mind that there is no standard setup for this type of operation and some systems can differ a lot from this description. Figure 3-6 shows a simple drawing of the system [19]. Here each partition is connected directly to each other through pipes called equalizers. This is done for two reasons, first to avoid synchronization problems when the mud pump is turn on or off like during a pipe connection procedure. The drilling mud in this instance will flow back through the equalizers and avoid overfilling the tanks. The other reason is to guarantee that there will always be drill fluid inside the last tank which is sometimes refer to as the active pit and is the partition that provide drill mud to the mud pump. If the mud pump is unable to pump drill mud into the well, this will cause the pressure to decrease which could cause a blowout.

Here is a step by step explanation of this system:

1. The drill fluid flows from the return line to the shale shaker which is situated on the top of the first mud tank. Most the solids are remove in this stage. The first tank has a sand trap and the overflow from this tank will flow into the next letting smaller insoluble particles lay on the bottom.
2. From the second tank, the drill fluid is pumped into a degasser to remove gas bubbles. The drill fluid will flow from the degasser into the third tank. Overflow from the third tank will flow back into the second tank. Figure 3-6 shows an extra tank (the third tank), this will not always be present and some systems skip this. The third and fourth tank are connected at the bottom so they will have the same level.
3. From the fourth tank, the drill fluid is pumped into a mud cleaner and into the fifth tank. The fourth and fifth tank are connected at the bottom and the underflow from the fifth tank will flow back into the third tank. In this stage, the system can differ depending on the equipment use. Instead of a mud cleaner, some systems have distillers and desander, a combination of the three or in some cases none of them.
4. From the fifth tank, part of the drill fluid is pumped into a centrifugal desander to remove the smallest cuttings. Another part of the drill fluid will flow directly from the fifth to the last tank (the active pit). Some system will have more tanks connected in series as part of the additive section. From the active pit the mud is pumped back into the well.

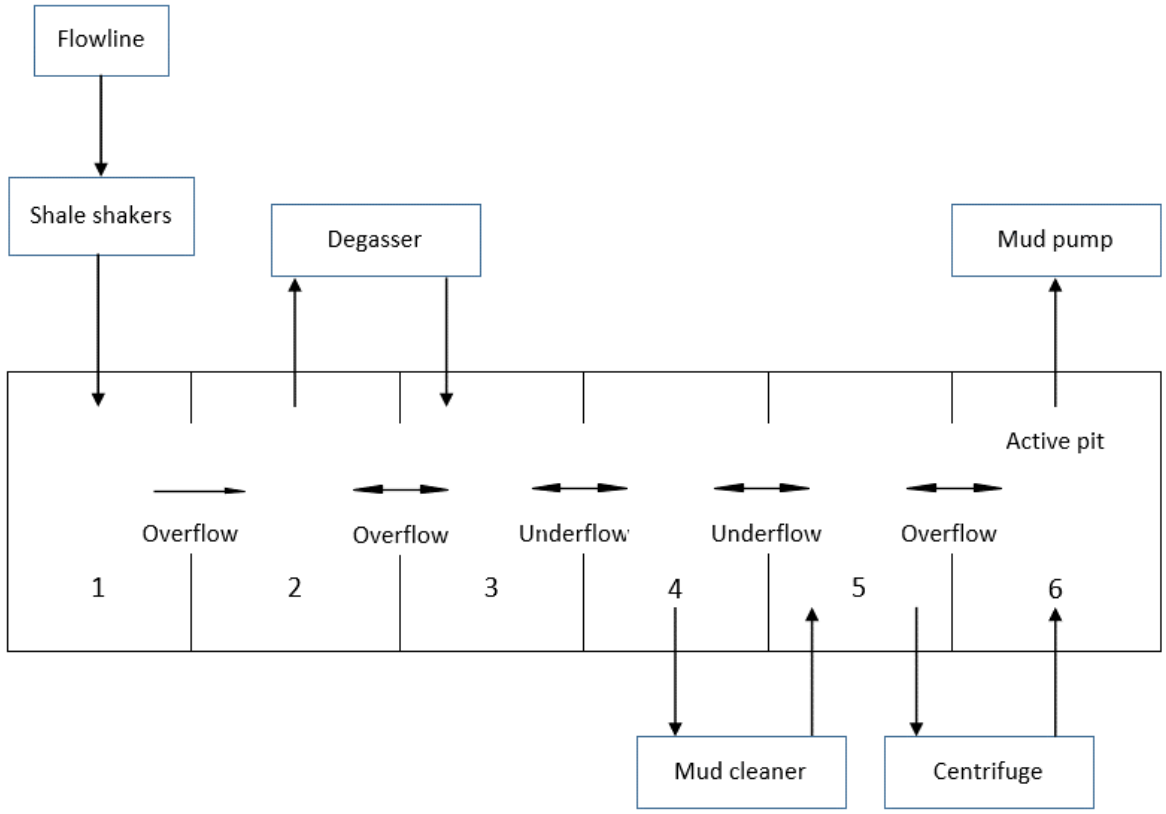

Figure 3-6 Overview of a solid control system

3.4 Fluid losses through the system

Losses though the solid control system are very difficult to quantify. Fluid losses are normally documented. However, these reports do not separate the losses cause by the solid removal equipment and losses caused by over-balanced drilling.

If one assumes that there are no losses thought the system because of leakage, all the losses in the circulation will be caused by the fluid retention on cuttings disposed by the solid removal equipment.

Figure 3-7 Waste from a shale shaker [20]

The volume of drill cuttings generated depends primarily on the size of the well drilled. It also depends on the type of formation being drilled, the type of drill bit and the properties and type of drilling mud used. At the same time the volume of solids retrieved from the well depend on the flow from the mud pump and the viscosity of the drilling fluid. [21]

The solids removed from the system will not be completely dry and part of the drilling fluid will be dispose along with the waste. The amount of drill fluid loss depends on the efficiency of the solid removal system, the type of drilling fluid used and the size of the cuttings. The API has published guidelines of how to measure the drill fluid content from cuttings by retort analysis (API RP 13B-2). This value is normally between 5 to 15% by weight. Note that since the density of the cuttings is higher than the density of the drill mud, the percentage of loses by volume will be higher. The Environmental Protection Agency conducted a study to analyze the drill fluid retention on cutting on 65 wells for different types of equipment (when present). Some averages include 9.32% for (primary) shale shakers, 9.97% for decanting centrifuges and 11.9% for mud cleaners. By using dryers, it can be further reduced to 4.84/3.82 % (depending on the setup). [21]

Taking some values from a case study performed by M-I SWACO to test the performance of one their products, a shale shaker use to remove solids from oil base drill muds [22]. The average pump rate was 517 gallons per minute, the average of oil left on cuttings measured by weight was 10.16% and the discard rate of solids was 4.16 lb./s. The density of the fluid was not given so is assume to be around 12 pounds per gallon.

To calculate the total weight of the fluid losses per minute:

$$m_L = 4.16 * 0.1016 * 60 = 25.36\ lb/min$$

Using this value one can calculate the losses in gallons per minute.

$$V_L = \frac{25.36}{12} = 2.11\ gpm$$

This is not a completely accurate estimate since it does not consider the losses in barite and other components of the drill fluid individually. However, this can give a general idea of the losses. This example also only take into consideration the losses through the primary shale shaker, but is also where most the losses are produce. If one assumes that the waste from the primary shale shakers represents around 80% of the total waste and there are no major differences in the retention of fluid on cuttings for the rest of the equipment, the total loses can be estimated to be around:

$$V_{LT} = \frac{2.11}{0.8} = 2.634\ gpm$$

The relevancy of these losses is dependent on the total amount of drill fluid circulating in the system and the operating hours of the rig.

4 Model development

The system can be simplified to consider the losses of the entire solid removal system instead of each individual equipment as the solid removal system has no standard arrangement and is too complex. Figure 4-1 show the simplified model. Here the flow delay through the solid removal system is neglected.

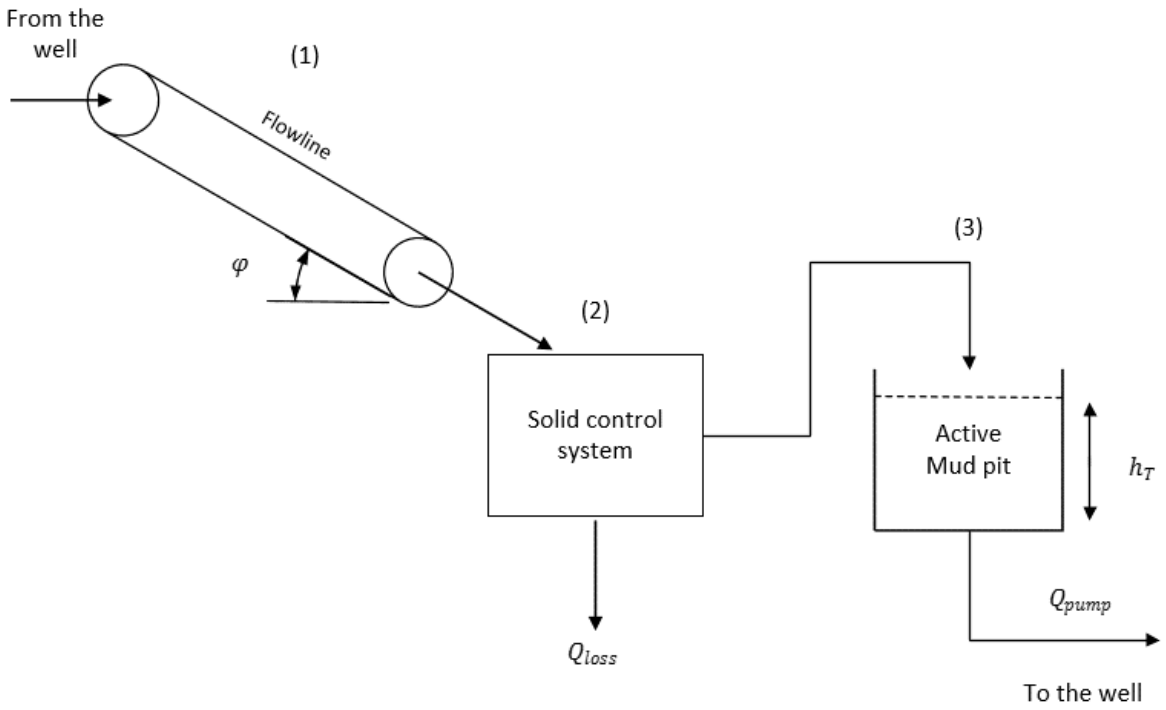

Figure 4-1 Simplified model for the drain back

First the drill mud will flow from the annulus through the choke valve into the flowline at (1). The flow through the flowline is open channel and the fluid will contain cuttings carried from the bottom of the well increasing its density. At this point, there are no fluid losses.

The mud will then flow into the solid removal system were the cuttings will be partially removed (2). This will change the density of the fluid depending on the efficiency of the solid removal system. There will also be losses depending on the discard rate of solids and the fluid retention on cuttings in the waste. Considering that there are no gasses in the drill fluid, one can write that:

$$\rho_a Q_{pipe} = \rho_{cl} Q_{cl} + \rho_{cl} Q_{loss} + \rho_{cu} Q_{cu} \quad (4.1)$$

Where $\rho_{cu} Q_{cu}$ is the mass flow of solids removed from the system, $\rho_{cl} Q_{cl}$ is the mass flow of the clean drill mud after the solid removal system and $\rho_{cl} Q_{loss}$ is the mass flow of the fluid losses out of the system. The output from the solid control system will be the mass flow of clean mud:

$$\rho_{cl} Q_{cl} = \rho_a Q_{pipe} - \rho_{cl} Q_{loss} - \rho_{cu} Q_{cu}$$

The clean fluid will finally flow into the active pit (3) where it will be pumped back into the well though the mud pump. The density of the fluid inside the tank will gradually change over time depending on the remaining cuttings and other possible fluids coming from the wellbore.

4.1 Frictionless case

For the frictionless case one can neglect the flow delay through the flowline. Looking at the contents of the active pit, using mass balance, one can derived the following equation:

$$Ar_{bT}\frac{d\rho_T h_T}{dt} = \rho_{in}Q_{in} - \rho_{out}Q_{out} \tag{4.2}$$

Where A_{bT} is the base area of the active pit and ρ_T and h_T the density and the level of the drill mud inside the tank. The flow going into the active pit can be taken from the RHS of equation 1.1. This is without considering any flows from the reserve pits.

$$\rho_{in}Q_{in} = \rho_a Q_{pipe} - \rho_{cl}Q_{loss} - \rho_{cu}Q_{cu}$$

The flow out of the system is equal to the flow being pumped by the mud pumps. Since the fluid inside active pit can be assumed to be well mix, one can write that the density of the drill mud pumped by the mud pump and the back-pressure pump is equal to the density of the fluid inside the active pit which consequentially will be equal to the density of the fluid pumped into the drill string.

$$\rho_{out}Q_{out} = \rho_d Q_{pump} + \rho_d Q_{back}$$

Combining the previous equations:

$$Ar_{bT}\frac{d\rho_d h_T}{dt} = \rho_a Q_{pipe} - \rho_{cl}Q_{loss} - \rho_{cu}Q_{cu} - \rho_d Q_{pump} - \rho_d Q_{back}$$

Using the chain rule:

$$Ar_{bT}\left(h_T\frac{d\rho_d}{dt} + \rho_d\frac{dh_T}{dt}\right) = \rho_a Q_{pipe} - \rho_{cl}Q_{loss} - \rho_{cu}Q_{cu} - \rho_d Q_{pump} - \rho_d Q_{back} \tag{4.3}$$

Assuming 100% efficiency of the solid removal system This will mean that there are no changes in the density and one can write that the density of the clean drill mud will be always constant and equal to the density of the fluids inside the active pit/drill string.

$$\rho_{cl} = \rho_d$$

Also, ignoring the flow dynamics of the solid control system:

$$\rho_d Q_{pipe} = \rho_a Q_{pipe} - \rho_{cu}Q_{cu}$$

$$\frac{dh_T}{dt} = \frac{1}{Ar_{bT}}(Q_{pipe} - Q_{loss} - Q_{pump} - Q_{back}) \tag{4.4}$$

Here the change in the fluid level of the tank will be caused by the losses in the solid removal system, the volume change of the annulus and drill string (calculated only after a pipe connection procedure) and the flows from the reservoir.

$$Q_{pipe} - Q_{pump} - Q_{back} = -\dot{V}_a - \dot{V}_d - Q_{loss} + Q_{res}$$

$$\frac{dh_T}{dt} = \frac{1}{Ar_{bT}}(-\dot{V}_a - \dot{V}_d - Q_{loss} + Q_{res}) \quad (4.5)$$

The fluid losses and the mass of the drill cuttings can be estimated using the rate of penetration of the drill bit:

$$m_{cu} = \frac{\pi D_w^2}{4}\frac{dh_{bit}}{dt}s_{fr}$$

$$m_{loss} = \frac{\%retention\ on\ cuttings}{1 - \%retention\ on\ cuttings}m_{cu}$$

Where D_w^2 is the diameter of the well, dh_{bit} is the change in height of the drill bit and s_{fr} is the solid fraction. Since the fluid level in the tank is measurable, this will leave Q_{res} as the only unknown value.

In practice, the solid removal system will not be able to remove all the cuttings from the fluid. This will gradually increase the density of the drill mud inside the active pit. From equation 4.3 solving with respect to the change in density gives:

$$\frac{d\rho_d}{dt} = \frac{\rho_{cl}Q_{pipe} - \rho_{cl}Q_{loss} - \rho_d Q_{pump} - \rho_d Q_{back}}{Ar_{bT}h_T} - \rho_d\frac{dh_T}{dt} \quad (4.6)$$

Where:

$$\rho_{cl}Q_{pipe} = \rho_a Q_{pipe} - \rho_{cu}Q_{cu}$$

5 Flow through prismatic open channels

The flow going through the flowline is assumed to be open channel. This means that the fluid going through the pipe will always have a free surface were the pressure is equal to the atmospheric pressure. The most common way to represent the dynamics of these type of flows is with the help of the Saint Venant equations. These are a set of partial differential equations derived by the French engineer Adhémar Barré de Saint-Venant in 1871. [23]

Consider a channel with length L (as showed in figure 5-1), an incompressible fluid flows through the channel with a cross-sectional A (as showed in figure 5-2).

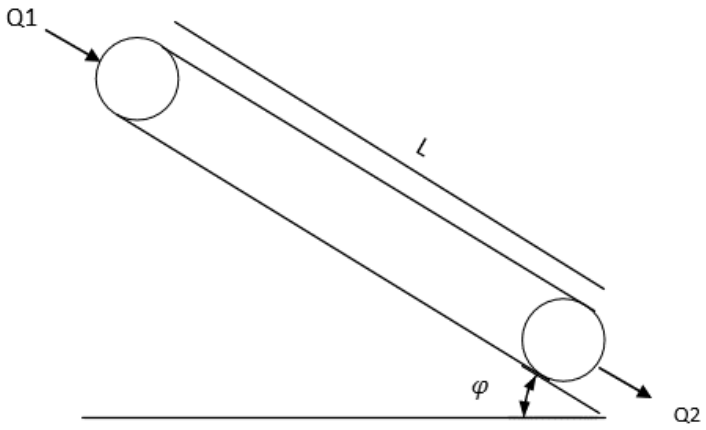

Figure 5-1 Channel elevation

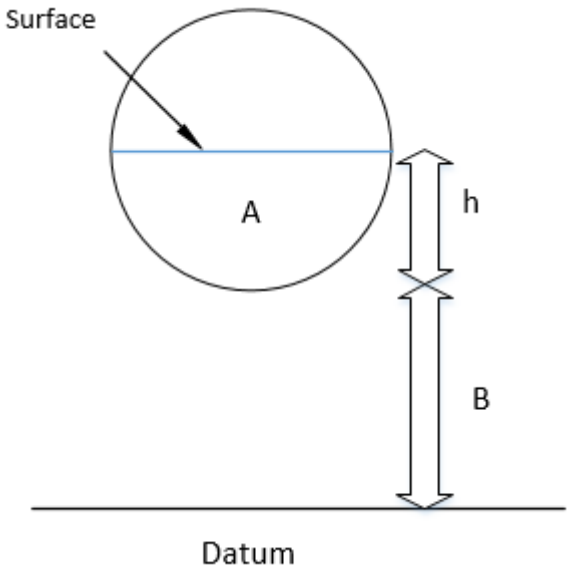

Figure 5-2 Cross-sectional area of the flow

The slope of the channel is equal to the change in the channel elevation:

$$S_0 = -\frac{\partial B}{\partial x} \tag{5.1}$$

Where *B* is the elevation at the bottom of the pipe with respect to a datum.

The volumetric discharge from the pipe will change with respect to time and length. Following the law of conservation of mass, the partial derivative of the discharge with respect to the length will be equal to the flow going into the channel minus the flow out of the channel.

$$\frac{\partial Q}{\partial x}\Delta x = Q_2 - Q_1$$

There will also be a change in volume along the pipe with respect to time:

$$\frac{\partial A}{\partial t}\Delta x$$

These two terms are of equal magnitude and different sign, combining the two will give thus the first of the Saint Venant equations for one dimensional flow, the so-called continuity equation.

$$\frac{\partial Q}{\partial x} + \frac{\partial A}{\partial t} = 0 \tag{5.2}$$

For the momentum equation one can start by using Newton's second law, that dictates that the sum of the forces working on the fluid is equal to the mass times the acceleration:

$$\sum F = \rho A \Delta x \frac{dv}{dt}$$

The forces working on the fluid are a frictional resistance of the channel, a force done by the change in static pressure and a gravitational force. The friction force is working along the pipe and can be represent as follows:

$$F_f = -\rho g \Delta x A S_f$$

Here S_f is the friction term. The change in static pressure is working horizontally and can be represent as:

$$\frac{\partial H}{\partial x} = -\rho g \Delta x I cos(\varphi)$$

I is the hydrostatic pressure of the fluid equal to:

$$I(x, A) = \int_0^{h(x,A)} (h(x, A) - \tilde{z}) w(x, \tilde{z}) dz \tag{5.3}$$

At last there is a gravitational force working downwards which can be written as:

$$G = \rho g \Delta x A \sin(\varphi)$$

Assuming that the slope of the channel is small like in the case of most rivers, this can be further simplified as:

$$\sin(\varphi) \approx \tan(\varphi) = S_0$$

$$\cos(\varphi) \approx 1$$

Combining the equations:

$$\rho A \Delta x \frac{dv}{dt} = -\rho g \Delta x I - \rho g \Delta x A S_f + \rho g \Delta x A S_0$$

The velocity term *v* will vary with respect to time and length therefore:

$$\rho A \Delta x \left(v \frac{\partial v}{\partial x} + \frac{\partial v}{\partial t} \right) = -\rho g \Delta x I - \rho g \Delta x A S_f + \rho g \Delta x A S_0$$

Simplifying this will give thus the momentum balance of the Saint Venant equation:

$$\frac{\partial Q}{\partial t} + \frac{\partial}{\partial x}\left(\frac{Q^2}{A} + gI \right) = gA\left(S_0 - S_f\right) \tag{5.4}$$

For uniform flow of Newtonian fluids in channels of simple cross section, the friction term S_f can be represented by using the manning's equation.

$$Q = \frac{1}{n} A R^{2/3} S_f^{1/2}$$

$$S_f = \frac{Q|Q|n^2}{A^2 R^{\frac{4}{3}}} \tag{5.5}$$

Where n is the manning's roughness coefficient and R the hydraulic radius equal to the cross-sectional area of the flow divided by the wetted perimeter.

$$R = \frac{A}{P_w}$$

5.1 Implementation of the Saint Venant equations to model the flowline

The return line is the pipe connecting the choke valve (or the choke manifold from the blowout preventer system) to the solid control system and is often called just flowline in the industry. It is normally just a common circular bore pipe and is normally treated just as a connector between the solid control system and the choke valve. The dimeter of such pipes ranges between 12 to 27 inches and the length can vary between several meters like in a normal onshore installation or several kilometers like for some offshore installations were a mud lift pump is used to circulate the pump back to the surface. [24]

For the purposes of this project, the flowline is assumed to be one pipe line section with a constant circular cross-sectional area and a relative small inclination. The continuity equation can be taken directly from equation 5.2.

$$\frac{\partial Q}{\partial x} + \frac{\partial A}{\partial t} = 0 \tag{5.6}$$

Since the pipe has a constant circular cross-sectional area, the hydrostatic in equation 5.3 can be written as:

$$I(A) = \int_0^{h(A)} (h(A) - \tilde{z}) w(\tilde{z}) dz$$

Where the width of the flow through a circular pipe with respect to the level of the flow and the dimeter of the pipe can be written as follows:

$$w(\tilde{z}) = 2\sqrt{\tilde{z}D - \tilde{z}^2}$$

A simplified solution for this is found in [25]:

$$I = \frac{1}{12}\left[(3D^2 - 4Dh + 4h^2)\sqrt{h(D-h)} - 3D^2(D-2h)\arctan\frac{\sqrt{h}}{\sqrt{D-h}}\right] \tag{5.7}$$

The slope of the pipe can also be too big to be simplified. The momentum equation will be as follows:

$$\frac{\partial Q}{\partial t} + \frac{\partial}{\partial x}\left(\frac{Q^2}{A} + gI\cos(\varphi)\right) = gA\sin(\varphi) - gAS_f \tag{5.8}$$

Combining equations (5.6) and (5.8), they can be written as follows

$$\frac{\partial U}{\partial t} + \frac{\partial F}{\partial x} = S \tag{5.9}$$

Where the *U* vector is the vector of conserved variables

$$U = (A, Q)^T$$

F is the vector of fluxes:

$$F = \left(Q, \frac{Q^2}{A} + gI_1\cos(\varphi)\right)^T$$

And S is the source terms:

$$S = \left(0, gA\sin(\varphi) - gAS_f\right)^T$$

Where the friction term be estimated using manning's equations (eq. 5.5).

The equations for calculating the cross-section area, the free surface and the wetted parameter are described in Appendix B.

5.2 Second order Central Upwind scheme

The Saint Venant equations cannot be solved explicitly. For the purposes of this thesis, a numerical scheme known as the Kurganov-Petrova central upwind scheme was implemented to solve the Saint Venant equations. Here just a list of equations use for this scheme is presented, for more details about this scheme refer to [26].

A way to solve the equations presented in the previous subchapter is using control volumes or cells. These are fixed volumes which the fluid flow through. Here one focuses in studying the masses that go through these cells.

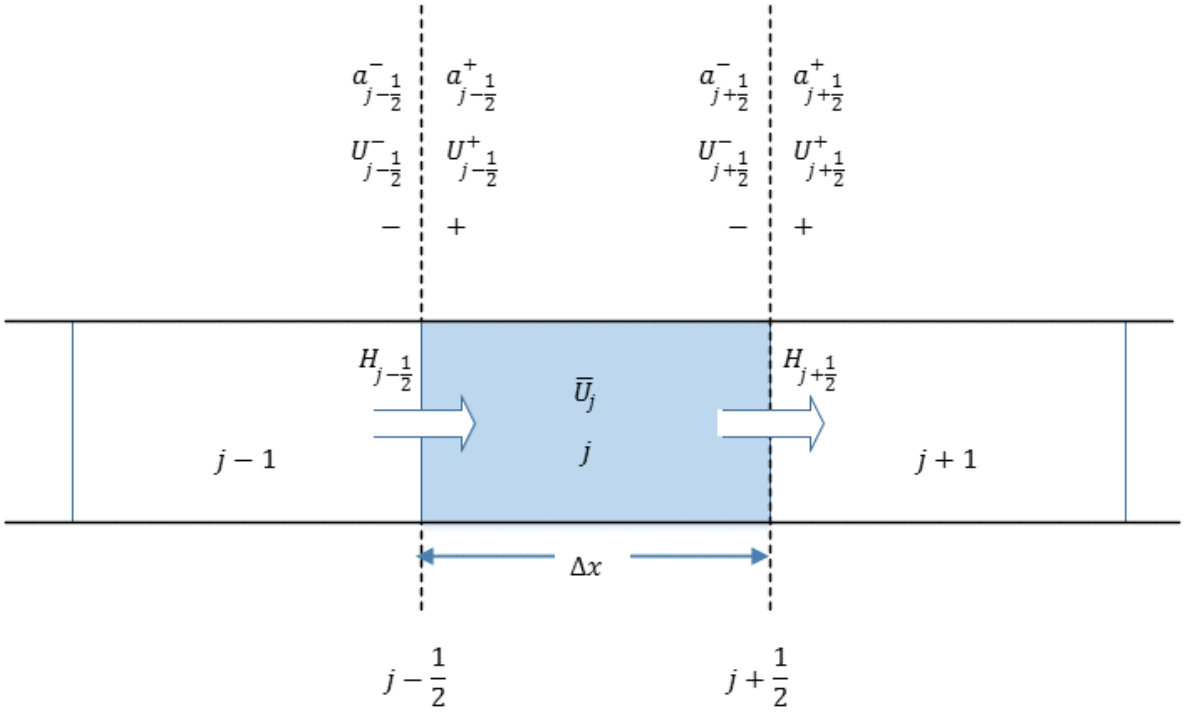

Figure 5-3 Control volumes/cells [26]

Where j is the cell number and $\overline{U}_j$ the average values of the conserved variables. Here there are values for the conserved variables at the start of the cell and at the end of the previous cell and at the end of the cell and the start of the current cell. a denotes the local speed propagations and Δx is the length of the control volume.

The cell average at a time $t = t_n$ will be as follow:

$$\overline{U}_j^n = \frac{1}{\Delta x}\int_{x_{j-\frac{1}{2}}}^{x_{j+\frac{1}{2}}} U(x, t_n)dx$$

For equation 5.9 this can be solved as:

$$\frac{d}{dt}\overline{U}_j = -\frac{H_{j+\frac{1}{2}}(t) - H_{j-\frac{1}{2}}(t)}{\Delta x} + \bar{S}_f(t) \tag{5.10}$$

Where

$$H_{j+\frac{1}{2}}(t) = \lim_{\Delta t\to 0}\frac{1}{\Delta t}\int_{t_n}^{t_n+1} F\left(U\left(x_{j+\frac{1}{2}}, t\right)\right)dt$$

$$H_{j-\frac{1}{2}}(t) = \lim_{\Delta t\to 0}\frac{1}{\Delta t}\int_{t_n}^{t_n+1} F\left(U\left(x_{j-\frac{1}{2}}, t\right)\right)dt$$

$$\bar{S}_f(t) = \lim_{\Delta t\to 0}\frac{1}{\Delta t\Delta x}\int_{t_n}^{t_n+1}\int_{x_{j-\frac{1}{2}}}^{x_{j+\frac{1}{2}}} S dx dt \approx \frac{1}{\Delta x}\int_{x_{j-\frac{1}{2}}}^{x_{j+\frac{1}{2}}} S\big(U(x,t)\big)dx$$

Using the KP scheme, the central upwind numerical fluxes $H_{j\pm\frac{1}{2}}(t)$ are given by (with no changes in the bed slope):

$$H_{j+\frac{1}{2}} = \frac{a^+_{j+\frac{1}{2}}F\left(U^-_{j+\frac{1}{2}}\right) - a^-_{j+\frac{1}{2}}F\left(U^+_{j+\frac{1}{2}}\right)}{a^+_{j+\frac{1}{2}} - a^-_{j+\frac{1}{2}}} + \frac{a^+_{j+\frac{1}{2}}a^-_{j+\frac{1}{2}}}{a^+_{j+\frac{1}{2}} - a^-_{j+\frac{1}{2}}}\left[U^+_{j+\frac{1}{2}} - U^-_{j+\frac{1}{2}}\right]$$

$$H_{j-\frac{1}{2}} = \frac{a^+_{j-\frac{1}{2}}F\left(U^-_{j-\frac{1}{2}}\right) - a^-_{j-\frac{1}{2}}F\left(U^+_{j-\frac{1}{2}}\right)}{a^+_{j-\frac{1}{2}} - a^-_{j-\frac{1}{2}}} + \frac{a^+_{j-\frac{1}{2}}a^-_{j-\frac{1}{2}}}{a^+_{j-\frac{1}{2}} - a^-_{j-\frac{1}{2}}}\left[U^+_{j-\frac{1}{2}} - U^-_{j-\frac{1}{2}}\right]$$

Where the local speed propagations can be estimated as the larges and smallest eigen values of the Jacobian of the system:

$$a^+_{j\pm\frac{1}{2}} = \max\left\{u^+_{j+\frac{1}{2}} + \sqrt{g{h_d}^+_{j\pm\frac{1}{2}}},\quad u^-_{j+\frac{1}{2}} + \sqrt{g{h_d}^-_{j\pm\frac{1}{2}}},\quad 0\right\}$$

$$a^-_{j\pm\frac{1}{2}} = \max\left\{u^+_{j+\frac{1}{2}} - \sqrt{g{h_d}^+_{j\pm\frac{1}{2}}},\quad u^-_{j+\frac{1}{2}} - \sqrt{g{h_d}^-_{j\pm\frac{1}{2}}},\quad 0\right\}$$

Here h_d is the hydraulic depth equal to the cross-sectional area of the flow divided by the free surface. It is also important to mention that the cell averages are used to calculate the values at each side of the control volumes.

$$\widetilde{U}_j(x) = p(x), \qquad x_{j-\frac{1}{2}} < x < x_{j+\frac{1}{2}}$$

This estimate does not consider the changes in width of non-prismatic channels.

5.3 Subcritical, critical and supercritical flow

To simulate the model and assign the boundary conditions, it is important to understand the different types of open channel flow. There are three types of flow: subcritical flow, supercritical flow and critical flow. [27] The type of flow is dependent on the size of the slope and the Froude number that is the *"The non-dimensional ratio of the inertial force to the force of gravity for a given fluid flow"*. [28]

To explain this let us take the example of how to derive the Froude number for critical flow which is the dividing line between the subcritical flow and supercritical flow. The specific energy of a fluid flowing in an open channel is equal to the sum of its kinetic and potential energy per unit weight, relative to the channel bottom.

$$E = h + \frac{v^2}{2g} \tag{5.11}$$

The velocity can be express in terms of the cross-sectional area of the flow and the discharge:

$$v = \frac{Q}{A}$$

Inserting this into the previous equation will give:

$$E = h + \frac{Q^2}{2gA^2} \tag{5.12}$$

Finding the derivative of (5.12) with respect to the level:

$$\frac{dE}{dh} = 1 - \frac{Q^2}{gA^3}\frac{dA}{dh} \tag{5.13}$$

The change in the cross-sectional area is equal to the change in level time the free surface that is the length of the section of the fluid that is expose to the atmospheric pressure.

$$dA = dh * T$$

For rectangular channels, the free surface will be a constant equal to the width of the channel and for circular and trapezoidal channels it will be a variable dependent on the flow level.

For critical flow the derivative of the specific energy with respect on the flow lever will be equal to zero:

$$\frac{dE}{dh} = 0$$

$$1 = \frac{Q^2 T_c}{g A_c^3}$$

Which is also a way to formulate the Froude number, in this case it is equal to 1.

$$Fr = \frac{Q^2 T_c}{g A_c^3} \tag{5.14}$$

A more common formulation is that the Froude number is equal to the velocity of the flow divided by the wave velocity also called celerity.

$$Fr = \frac{v}{\sqrt{g \frac{A_c}{T_c}}} \tag{5.15}$$

The flow is critical when the velocity of the fluid is equal to the celerity, the flow is supercritical when the velocity of the fluid is larger than the celerity and the flow is subcritical when the velocity of the fluid is smaller than the celerity. At the same time:

- A Froude number less than one, means that the flow is subcritical.
- A Froude number equal to one, means that the flow is critical
- A Froude number higher than one, means that the flow is supercritical

The specific energy for subcritical flow will increase with a higher flow level, the opposite happens with supercritical flow and the specific energy will decrease with a higher flow level as showed in figure 5-4 which shows the specific energy as a function of the flow depth for a constant flow of 2500 liters per minute through a circular pipe with a dimeter of 0.5 meters. Based on the Froude number the flow will be subcritical with a depth around 0.13 meters.

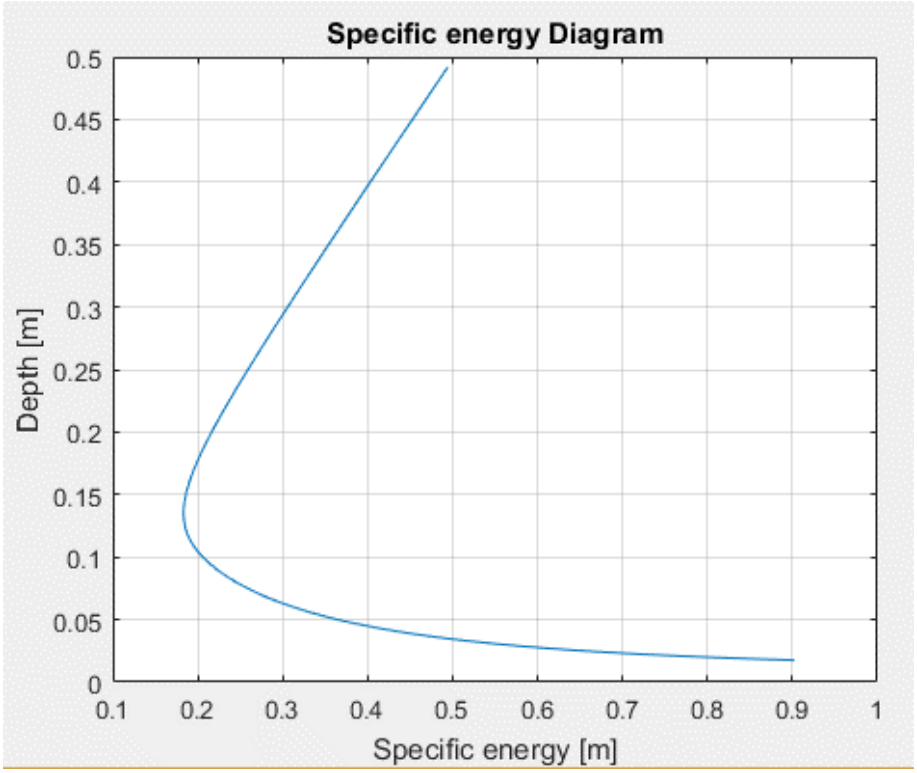

Figure 5-4 Specific energy diagram

6 Combined model

Summarizing the equations for the top and bottom side model. For the top side flow model:

$$\frac{V_d}{\beta_d}\dot{p}_p = Q_{pump} - Q_{bit} \tag{6.1}$$

$$\frac{V_a}{\beta_a}\dot{p}_c = Q_{bit} + Q_{back} - Q_{choke} + Q_{res} - \dot{V}_a \tag{6.2}$$

$$Mq_{bit} = p_p - p_c - F_d|Q_{bit}|Q_{bit} - F_a|Q_{bit} + Q_{res}|(Q_{bit} + Q_{res}) + (\bar{\rho}_d - \bar{\rho}_a)gh_{bit} \tag{6.3}$$

$$p_{bit} = p_c + M_a Q_{bit} + F_a|Q_{bit} + Q_{res}|(Q_{bit} + Q_{res}) + \bar{\rho}_a g h_{bit} \tag{6.4}$$

$$Q_{choke} = K_c z_c \sqrt{\frac{2}{\bar{\rho}_a}(p_c - p_0)} \tag{6.5}$$

Here the value of the discharge from the choke vale will work as the initial condition of the flowline. The flowline is divided into several control volumes, the changes in each control volume are calculated with the following equation:

$$\frac{d}{dt}\bar{U}_j = -\frac{H_{j+\frac{1}{2}}(t) - H_{j-\frac{1}{2}}(t)}{\Delta x} + \bar{S}_f(t) \tag{6.6}$$

where $\bar{U}$ is the average of the conserved i.e. the cross-sectional and the discharge of each control volume of the flowline. For a description of all the terms in this equation refer to subchapter 5.1 and 5.2.

$U = (A, Q)^T$

The discharge at the last control volume will be the value use to fill the active mud pit (Q_{pipe}):

$$\frac{dh}{dt} = \frac{1}{A_{bT}}\left(Q_{pipe} - Q_{loss} - Q_{pump} - Q_{back}\right) \tag{6.7}$$

Then the drill mud will be pumped from the active pit back into the drill string and the cycle will continue.

7 Simulation results for the combine model

Detailed simulations were performed to observe how the model will behave in some realistic scenarios. Focusing on the changes in the level of the mud pits and the delay caused by the flowline. The parameters used for bottom side model are the same defined on page 11 Table 2-1. In addition, there are other parameters related to the flowline and the mud pit. These are defined on table 7-1. For these simulations, there where assume no losses of drill fluid due to fluid retention on cuttings and 100% efficiency for the solid control system.

For the following simulations, the fluid is assumed to be Newtonian. This will not be the case a real system where the viscosity will be changing during operation.

Table 7-1 Parameters for the simulation of the flowline

Parameter	Value	Description	Unit
L	15	Length of the pipe	m
N_{Vd}	50	Number of segments	--
d	0.5	Diameter of the pipe	m
φ	7	Slope of the flowline	degrees
h_{pit}	2	Initial level of the mud pit	m
A_b	4	Base area of the mud pit	m^2
θ	1.3	dissipation tuner	--
n	0.04	Manning's roughness coefficient	--

7.1 Boundary conditions and initial values for the flowline

During a normal drilling operation, the mud pumps will be pumping drill fluid into the well and these will normally have high discharge rate of thousands of liters per minute. Because of these, it will be safe to assume that the flow flowing through the flowline will be either supercritical or trans-critical which means that the flow becomes supercritical at one point through the flowline.

Supercritical flows need two boundary conditions at the start of the first control volume and none at the end of the last control volume. In this case, it will need a starting value for the discharge and one for the cross-sectional area of the flow. Estimating the initial cross-sectional are of the flow at the start of the flowline, can be challenging. For the following simulations, the cross-sectional is unbounded, meaning that the simulation has only one boundary condition at the start which is the value for the discharge from the choke valve. Another scenario that was tested was using the diameter of the annulus as the initial cross-sectional area, the results for the discharge were seemly the same with both scenarios.

In a real operation, it is recommended to have a level sensor at the start of the flowline to get a boundary condition for the cross-sectional area and ensure more precise results.

7.2 Surge and swab scenario

Movements of the drill string will cause the discharge from the well to the choke valve to change. During swabbing the drill string is moved upwards from the well, this will decrease the discharge from the choke valve momentarily until the well is filled with drill mud. In contrast during surging, the drill string will be pushed downwards and into the well, this will cause a momentarily rise in the discharge from the choke valve.

For this simulation, the drill string was pulled from the well (swab) with a velocity of 18 meter per minute at 200 seconds and continue for 80 seconds. At 500 seconds, the drill string was pushed back into the well (surge) with the same velocity until the bit level was the same as at the start of the simulation. The discharge from the mud pump, the back-pressure pump and the opening of the choke valve were all keep constant though the simulation. The results from the changes on the lever of the fluid inside the mud pit are showed on figure 7-2.

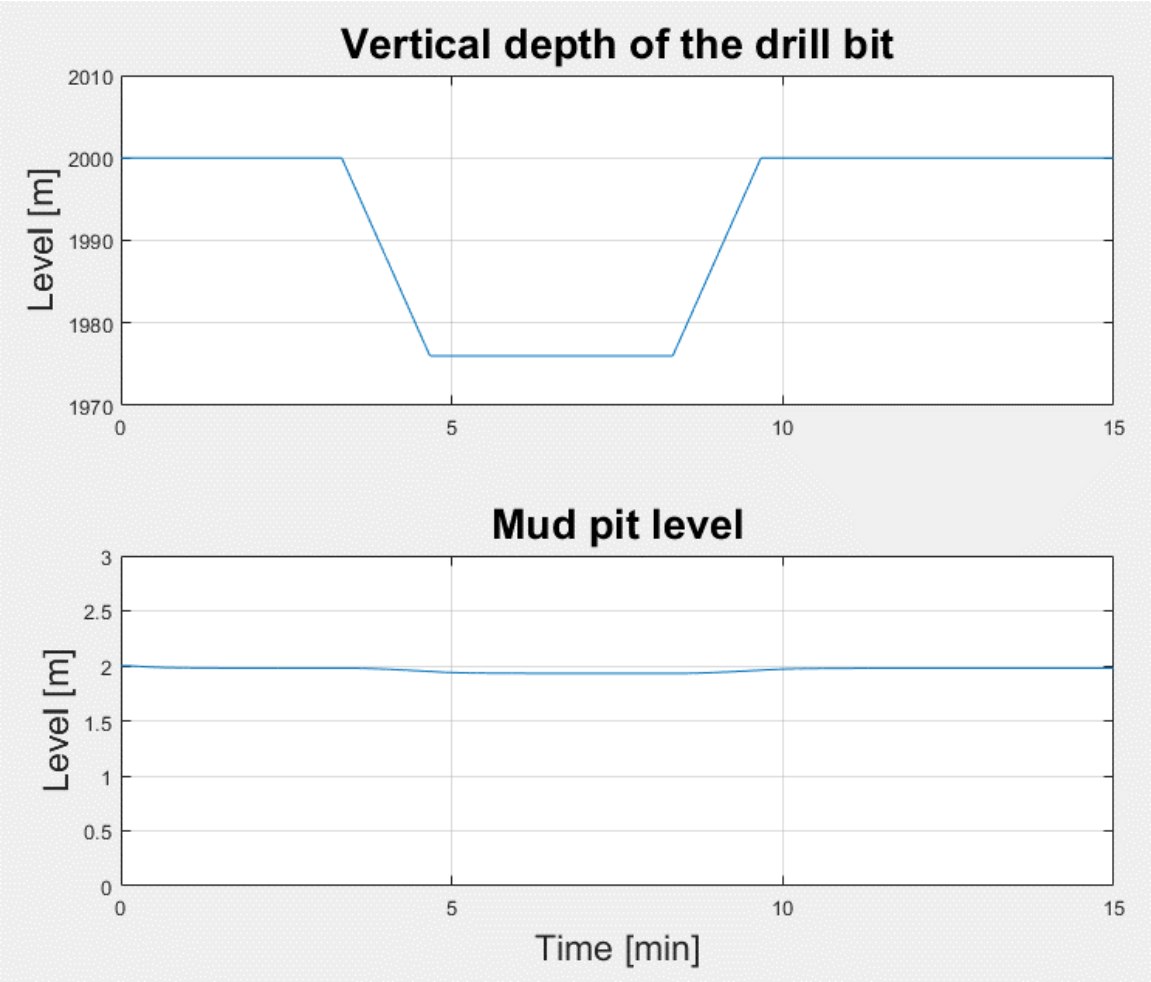

Figure 7-1 Change in the mud pit level due the movement of the drill string

The results show how the level of the mud pit decreased while pulling the drill string from the well and the opposite happens when the drill string is pushed back into the well. All this will happen after a delay dependent on length and the friction of the flowline. Using the values from table 7-1, there will be a delay of about 12 seconds before one can see any changes in the lever of the mud pit. This delay can also be observed while looking at the changes in the discharge at the start and at the end of the flowline showed in figure 7-2.

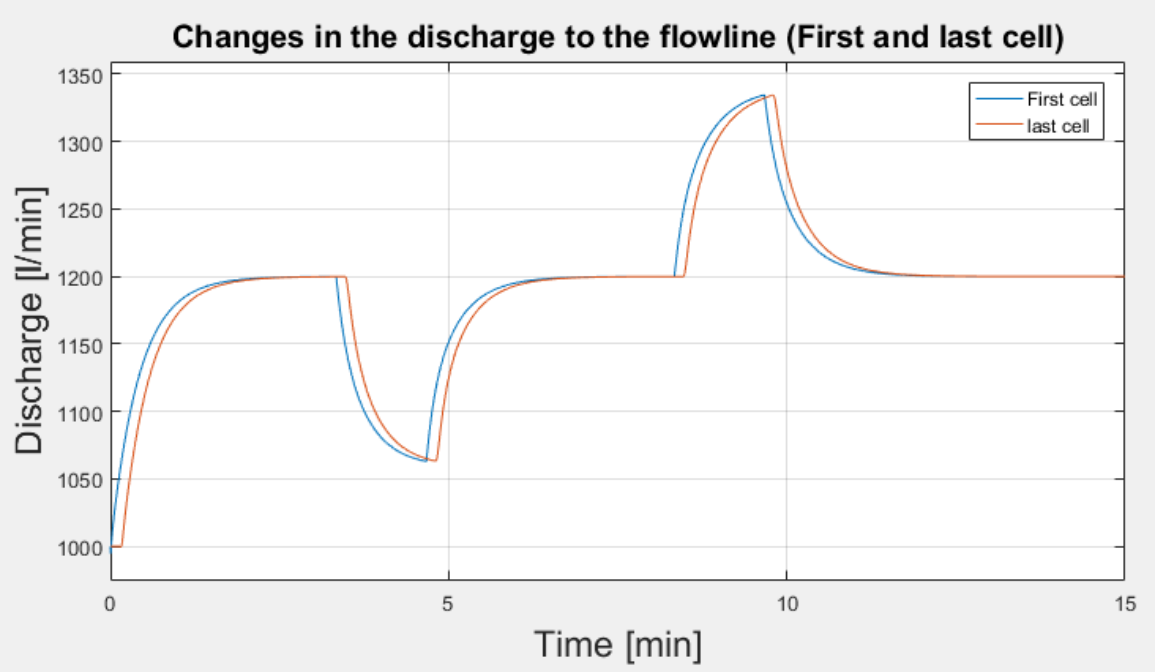

Figure 7-2 Changers in the discharge of the flowline during surge and swab

7.3 Influx from the reservoir scenario

A kick happens when flows enter the annulus from the reservoir. Here this is represented by the term Q_{res} on equation 6.2. A kick can be simulated by giving this term a positive value.

It is important to observe the delay that takes place after a kick and before the level increase of the mud pit. To test how the model will behave after a kick, two scenarios were tested. The first one is a step change where the flowrate from the reservoir change immediately from zero to 200 l/min and the second one the signal is ramped and it take 60 before the flowrate increases from zero to 200 l/min. The reasoning behind this two simulations is to see how much time will take before the change in the mud pit level is noticeable. Flows that enter the annulus from the reservoir after a kick are highly unpredictable so can be of interest to simulate different behaviors for this.

For these simulations, the backpressure pump was not in use and the discharge from the mud pump was keep constant. Figure 7-3 and 7-4 shows the changes of the mud pit level and the discharge through the flowline for the first simulation and figure 7-5 and 7-6 shows the changes of the mud pit level and the discharge through the flowline for the second simulation.

From these simulations is possible to see that there is a steady rise in the mud pit level and this can be used as an indicator that a kick has occurred. The differences in the delay of the two simulations is not very noticeable. As expected the ramped signal will give a larger delay, but the difference is very small.

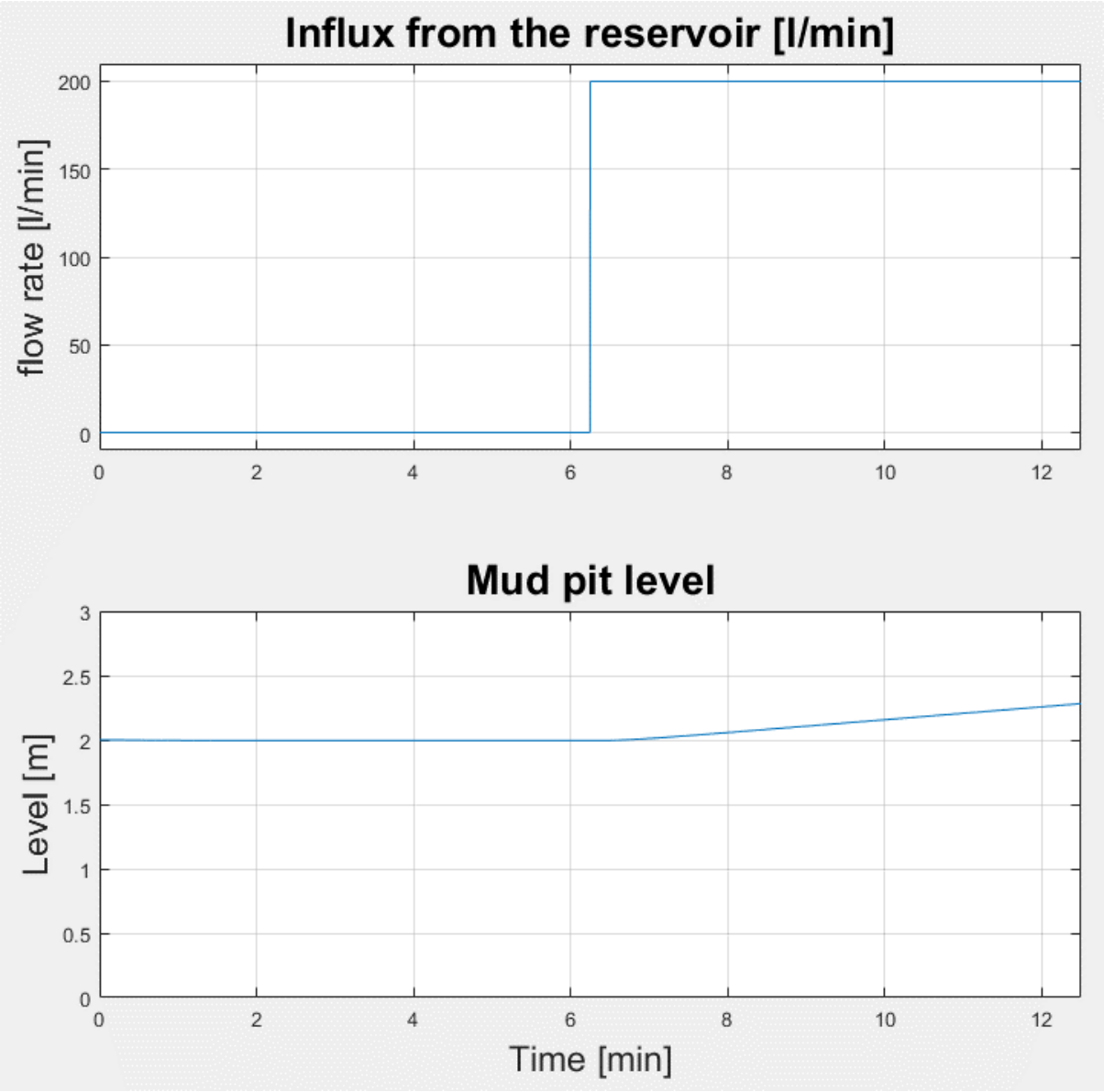

Figure 7-3 Changes in the mud pit level after an immediate influx from the reservoir

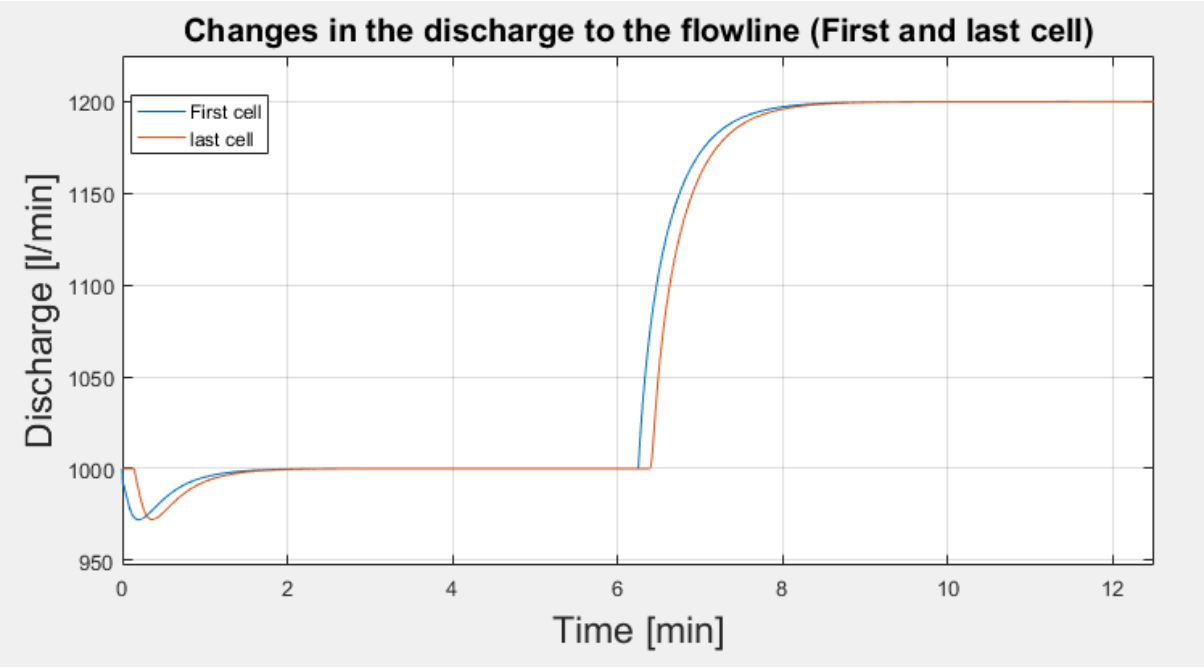

Figure 7-4 Changes in the discharge of the flowline after an immediate influx from the reservoir

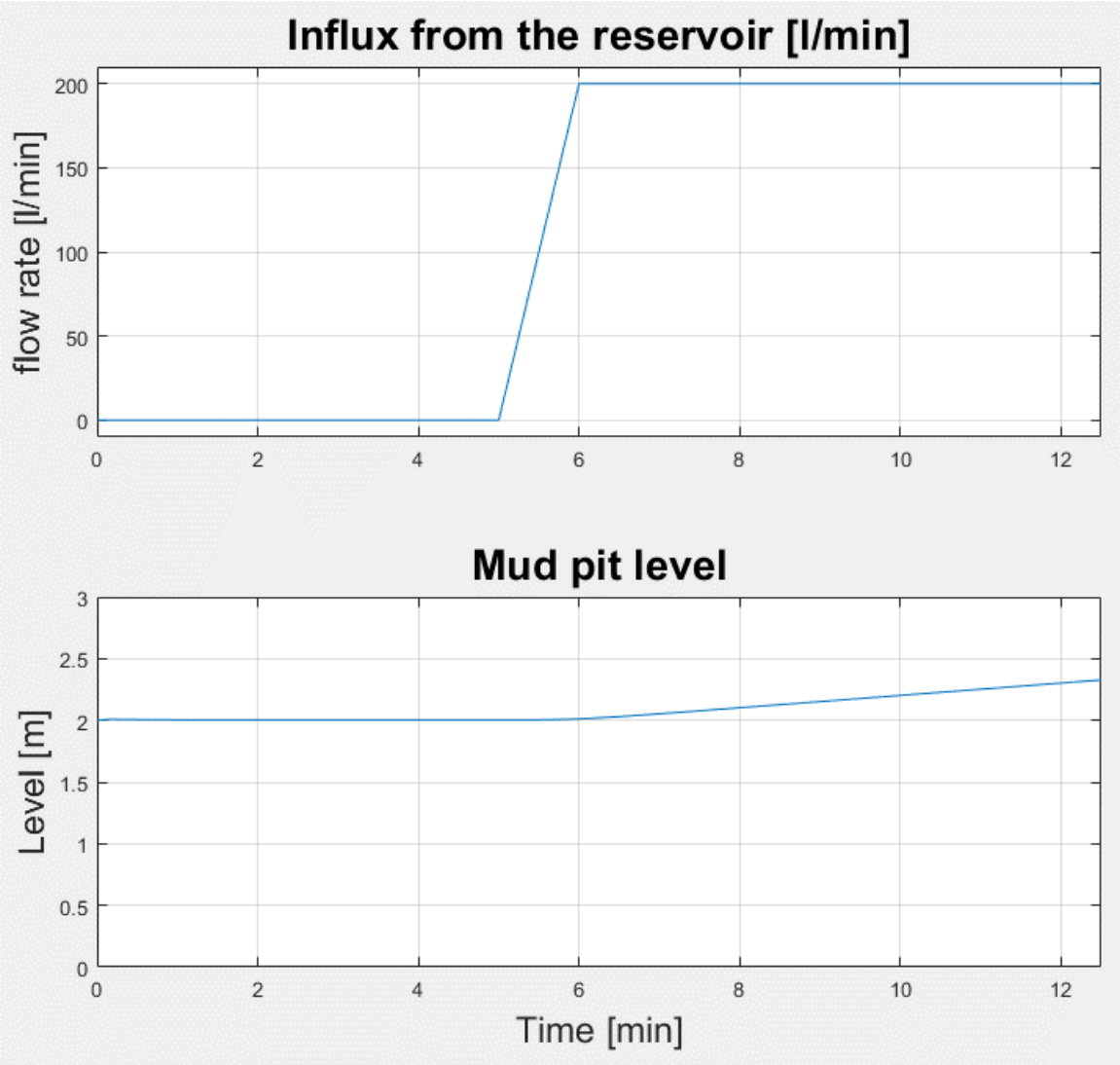

Figure 7-5 Changes in the mud pit level after a ramped influx from the reservoir

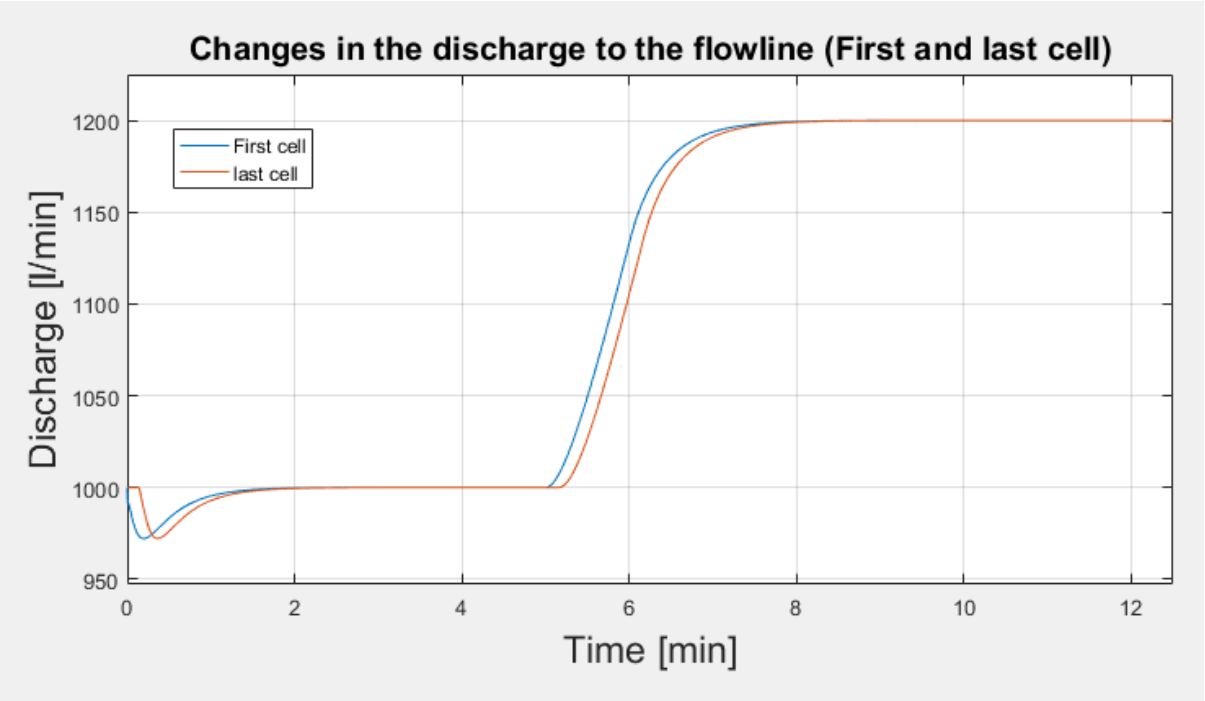

Figure 7-6 Changes in the discharge of the flowline after a ramped influx from the reservoir

7.4 Pipe connection procedure

During a pipe connection procedure, the mud pump will stop pumping drill fluid into the annulus. This will decrease the discharge from the choke valve and consequentially the discharge to the flowline. The KP scheme does not work with a zero-flow rate i.e. complete dry channel, thus the backpressure pump is used to have a non-zero flow rate in the flowline an also to manually maintain the bottom hole pressure.

For this simulation, the values for the opening of the choke valve, the backpressure pump and the mud pump were set manually and are showed in figure 7-7.

Figure 7-7 also shows the changes in the level of the mud pit. Here is possible to see than the level of the mud pit will increase slightly. This is due to the different rate of change of the inputs. Otherwise the changes are very minor.

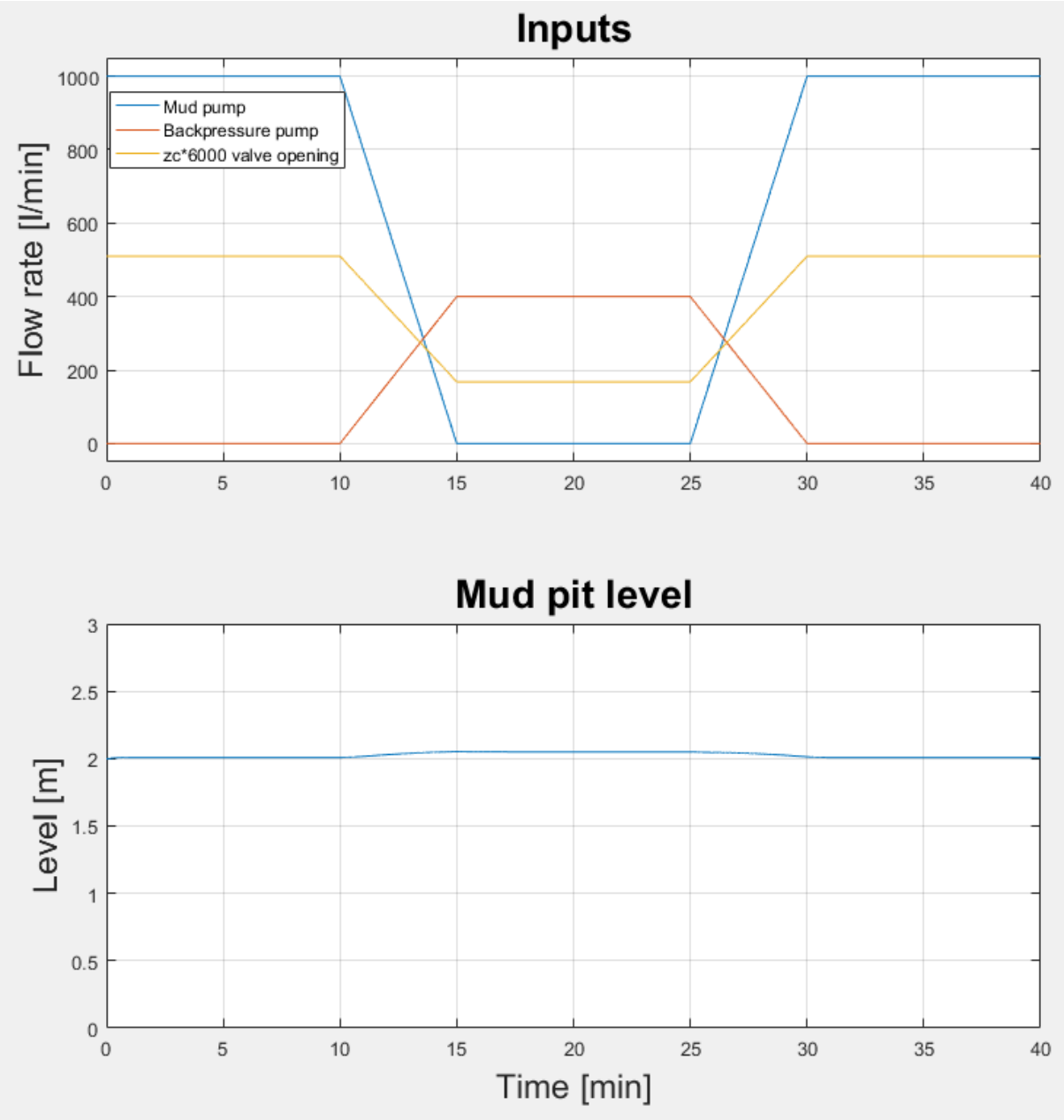

Figure 7-7 Changes in the mud pit level during a pipe connection procedure

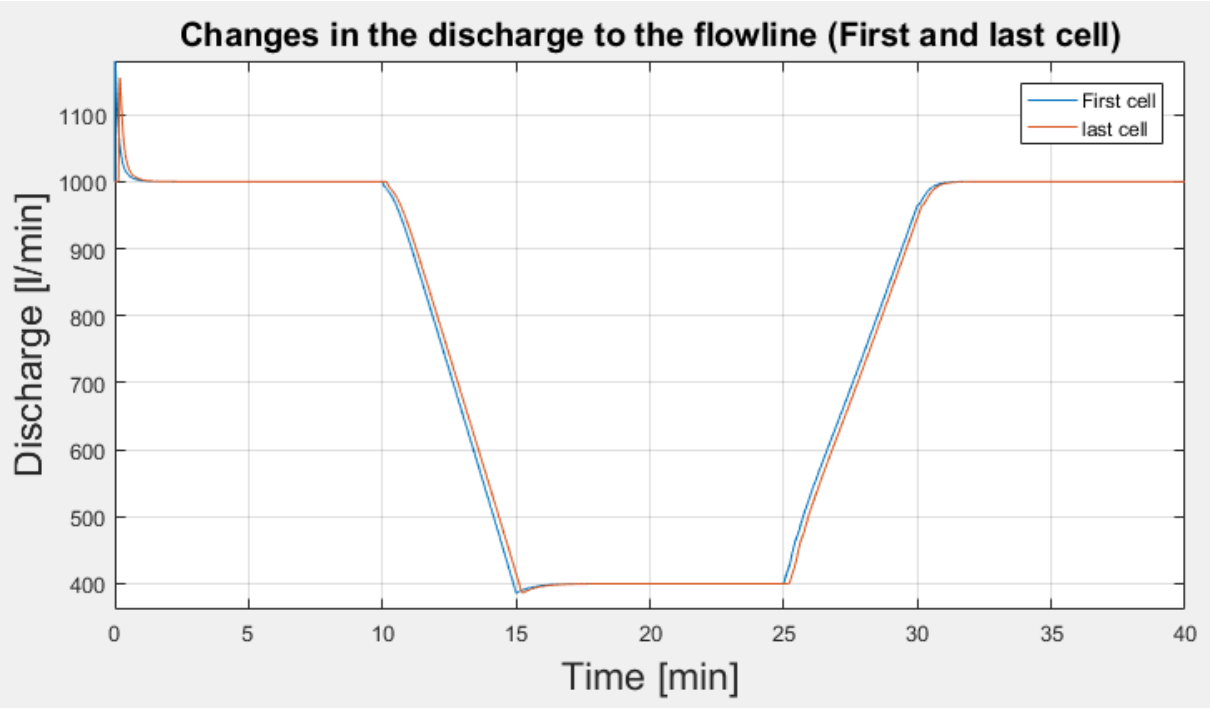

Figure 7-8 Changes in the discharges of the flowline during a pipe connection procedure

8 Discussion

This section is to discuss some of the possible limitations of the model.

8.1 Use of the model to estimate the density

In a drilling operation, the Coriolis meter has other uses on top of measuring the discharge through a flowline. It is also capable to measure the density and viscosity of the drill fluid. In order to replace the Coriolis meter, another method to measure the density needs to be implemented.

During a drilling operation, the density of the drill mud will be changing depending on the efficiency of the solid removal equipment. Theoretically a change in the density will also affect the volume of the drill fluid and therefore the level of the drill mud inside the mud pit. However, the changes will be very small, this combine with the fact that is not possible to correctly estimate all the fluid loses during a real operation (because of changes in the symmetry of the annulus, possible leakages during a pipe connection, etc.) it will be challenging to use the model to estimate the changes in density of the drill fluid.

8.2 Delay and kick detection

To successfully detect an influx or loss of fluid, the measurement of the change in flow from the mud pump to the return line needs to 50 gpm (190 l/min) or less [4]. It is important to study the delay caused by the solid control system to see if the prediction can still meet this requirement or if there needs to be another method to be used in conjunction with the model for early kick prediction.

Part II

Flow estimation using a Venturi flume

9 Flow estimation with a Venturi flume

One possibility to measure the flow from the return line and to replace the Coriolis meter is by using a Venturi flume. The use of these types of flumes is a common way to estimate fluid discharge of open channel flows. The challenge here is to test how precise the estimation is with a highly viscous fluid as the drill mud.

9.1 Overview of the Venturi flume

The university of South East Norway is equipped with a Venturi channel or flume which has multiple purposes, among them testing different techniques to estimate discharge, viscosity and density. The flume is most specifically a trapezoidal flume with a constant side slope, such types of flumes are normally used to measure flows through irrigations channels where the debris load in the stream can be expected to be high. [29]

Figure 9.1 shows a simple drawing of the flume.

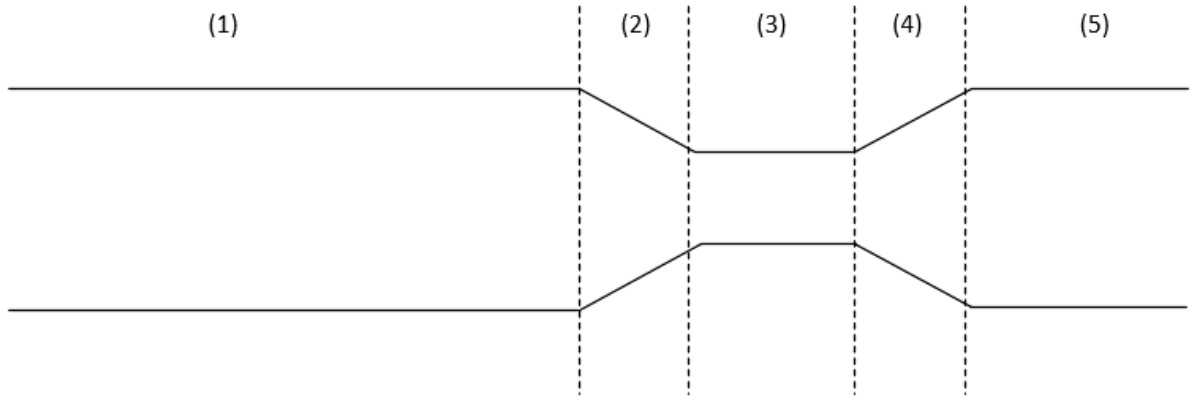

Figure 9-1 Geometry of the Venturi flume

The flume can be divided into five sections: (1) The upstream section, (2) converging section, (3) throat, (4) diverging section and (5) the downstream section. The side slope of the channel is constant in every section. The velocity of the flow increases as the flow passes the converging section, since the discharge will be constant the level of the flow will decrease.

Table 9-1 shows the dimensions of the flume.

Table 9-1 Parameters of the Venturi flume

Parameter	Value	Description
B_T	0.455	Top width of the upstream section [m]
B_*	0.355	Top width of the throat section [m]
b_0	0.2	Bottom width of the upstream section [m]
b_{*0}	0.1	Bottom width of the throat section [m]
H	0.35	Total height of the channel [m]
α	70	Slope of the sides of the channel [degrees]
L_a	2.95	Length of the upstream section [m]
L_b	0.15	Length of the converging section [m]
L_c	0.2	Length of the throat section [m]
L_d	0.15	Length of the diverging section [m]
L_e	0.25	Length of the downstream section [m]
L_T	3.7	Total length of the channel [m]

Such types of flumes normally use sensors to measure the level of the flow right before the converging section of the flume and at the throat and then use the Bernoulli's equation to estimate the discharge.

9.2 Bernoulli's equation for calculating the flow discharge

The Bernoulli's equation shows the relation between pressure and the potential and kinetic energy of an incompressible fluid where other external forces (like frictional forces) can be neglectable. [30]

Looking at figure 9-2, a force is applied to a fluid inside a tube or a channel and it will plush the fluid to a certain distance. The same will happen at the other side of the channel, depending on the dimensions of the channel there will be a change in the force and the distance traveled by the fluid.

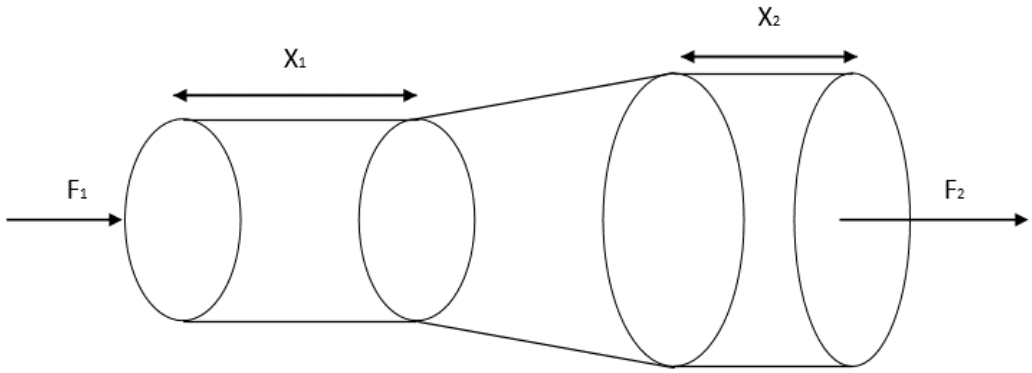

Figure 9-2 Fluid displacement in a channel

Neglecting the friction, the change in the work would be equal to the difference between the two:

$$\Delta W = F_1 x_1 - F_2 x_2 \quad (9.1)$$

Where the force at each side is equal to the cross-sectional are of the flow times the pressure:

$$F_1 = P_1 A_1$$

For incompressible liquids, the volume of the displaced fluid that is equal to the distance times the cross-sectional area will always be constant.

$$V = A_1 x_1 = A_2 x_2$$

The resulting equation for the work will be as follows:

$$\Delta W = (P_1 - P_2) * V \quad (9.2)$$

Using the energy balance and looking only in the changes of potential and kinetic energy:

$$\Delta E = E_1 - E_2 \quad (9.3)$$

$$\Delta E = mgh_1 + \frac{1}{2}mv_1^2 - \left(mgh_2 + \frac{1}{2}mv_2^2\right) \quad (9.4)$$

The work-energy theorem states that the work done by all forces acting on a particle equals the change in the particle's kinetic energy. This means that the change in the work is equal to the change in the system energy:

$$\Delta W = \Delta E$$

Combining equations 9.2 and 9.4:

$$(P_1 - P_2) * V = mgh_1 + \frac{1}{2}mv_1^2 - \left(mgh_2 + \frac{1}{2}mv_2^2\right)$$

This formula is most commonly written as follows:

$$P_1 + \frac{1}{2}\rho v_1^2 + \rho g h_1 = P_2 + \frac{1}{2}\rho v_2^2 + \rho g h_2 \quad (9.5)$$

This will be true for any two points in a single streamline. One can write that:

$$P_1 + \frac{1}{2}\rho v_1^2 + \rho g h_1 = constant \quad (9.6)$$

To find the discharge, one must also note that the discharge will be constant through the channel:

$$Q_1 = Q_2$$

$$A_1 v_1 = A_2 v_2 \quad (9.7)$$

Solving with respect of the velocity at the second point:

$$v_2 = \frac{A_1}{A_2} v_1 \quad (9.8)$$

Inserting equation 9.8 into 9.5

$$P_1 + \frac{1}{2}\rho v_1^2 + \rho g h_1 = P_2 + \frac{1}{2}\rho \left(\frac{A_1}{A_2} v_1\right)^2 + \rho g h_2$$

For open channel flow, the pressure will always be equal to the atmospheric pressure and therefore can be taken out of the equation. The density is constant so it can also be taken out of the equation and this leave:

$$\frac{1}{2}v_1^2 + g h_1 = \frac{1}{2}\left(\frac{A_1}{A_2} v_1\right)^2 + g h_2$$

Solving the equation with respect to the velocity at the first point:

$$v_1 = \sqrt{\frac{2g(h_1 - h_2)}{\left(\frac{A_1}{A_2}\right)^2 - 1}} \quad (9.9)$$

Multiplying with the cross-sectional are will give as the result, the discharge of the system.

$$Q = A_1 \sqrt{\frac{2g(h_1 - h_2)}{\left(\frac{A_1}{A_2}\right)^2 - 1}} \tag{9.10}$$

However, Bernoulli's equation has the following restrictions:

- The flow must be steady
- The density is constant (the fluid is incompressible)
- Friction losses are negligible
- The two points must be along a single streamline

The third point is the most important here, since friction will always be present. The question becomes, how big must the friction term be before the estimation become too imprecise, and is there a way to compensate for this error?

10 Dynamic model of the Venturi flume

A model of the flume was developed to have a better understanding of how the flow behaves through the Venturi channel and to try to find different ways to estimate the discharge. There are two important aspects with this flume. First the flume has a trapezoidal cross-sectional area with constant side slope, and second the channel is non-prismatic. The equations related to flow through trapezoidal channel are showed in the Appendix C. The continuity equation is the same as in equation 5.2:

$$\frac{\partial Q}{\partial x} + \frac{\partial A}{\partial t} = 0 \tag{10.1}$$

The term that represents the hydrostatic pressure taken from equation 5.3 and solve for trapezoidal channels is the following:

$$I_1 = h^2\left(\frac{W}{2} + h\frac{S_L}{3}\right) \tag{10.2}$$

Where W is the width of the base of the channel and S_L the side slope. Because the system is non-prismatic, there another term for the changes in the hydrostatic pressure due to the width variations [26]:

$$I_2(x, A) = \int_0^{h(x,A)} (h(x, A) - \tilde{z})\frac{\partial w(x, \tilde{z})}{\partial x} d\tilde{z}$$

For trapezoidal channels:

$$I_2 = h^2\left(\frac{1}{2}\frac{dW}{dx} + \frac{h}{3}\frac{dS_L}{dx}\right) \tag{10.3}$$

In this case, the side slope is always constant so this term will only depend on the changes in the base width. The momentum balance taken from equation 5.4 and including the new term for the hydrostatic pressure due to width variations:

$$\frac{\partial Q}{\partial t} + \frac{\partial}{\partial x}\left(\frac{Q^2}{A} + gI_1\right) = gI_2 + gA(S_0 - S_f) \tag{10.4}$$

The friction term can be estimated using the manning's equation just like with the previous model (equation 5.5 on page 30). The manning's roughness coefficient for the flume is not known so different values for it were tested.

Summarizing the model:

$$U = (A, Q)^T$$

$$F = \left(Q, \frac{Q^2}{A} + gI_1\right)^T$$

$$S = \left(0, gI_2 + gA(S_0 - S_f)\right)^T$$

10.1 Number of control volumes

Currently the way that the model works using the second order central upwind is the same as described in chapter 5.2. The model is divided into multiple control volumes which have two sets of values for the discharge and the cross-sectional at each side of the control volume. However, this does not compensate for the change in the cross-sectional area of the channel. This would not be a problem in cases where the change in width are not very big, however in this case the channel has a very abrupt change in the converging and diverging sections of the channel.

This is exemplified in figure 10-1 that show the discharges on each the control volumes after reaching steady state. Here the model was simulated with a discharge of 360 liters per minutes and with the length of each control volume equal to five centimeters. All the values for the discharges should be the same after reaching steady state and yet here the results show a big mismatch in some of the control volumes. The values that are farthest from the real discharge are the values from the start and end of the converging and diverging sections of the Venturi channel.

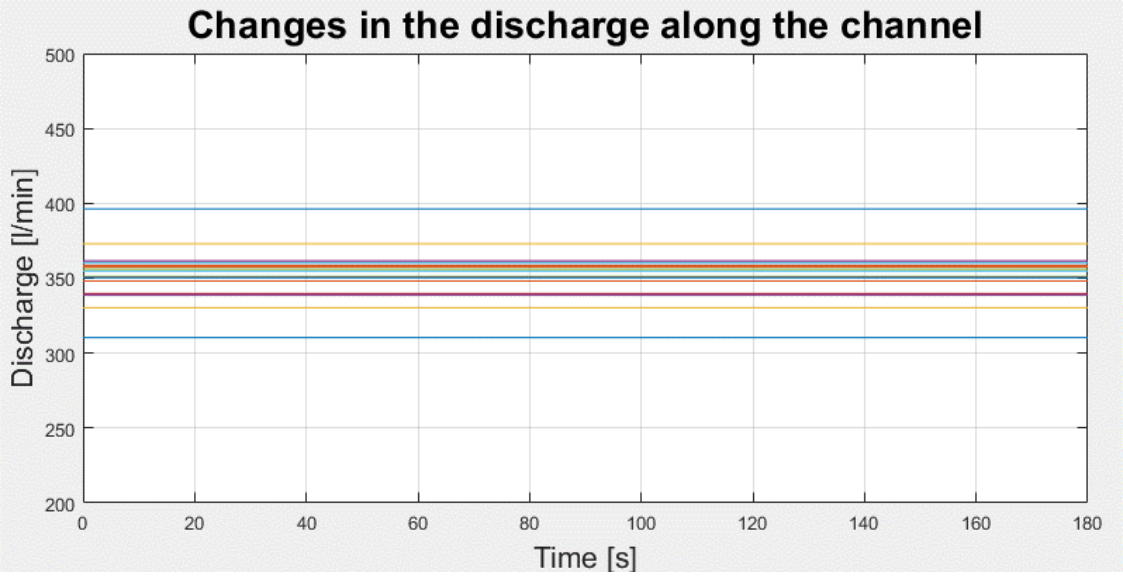

Figure 10-1 Discharges using control volumes with 5 cm in length

Increasing the number of control volumes by reducing the length of each of them, will reduce the disparities as showed in figure 10-2 where the length of the control volumes was reduced to 1 cm. However, as the number of control volumes increase so will the computation time.

Figure 10-3 shows how the size of the control volumes affects the level of the results. It is important to note that for these simulations the friction term was chosen to be very high. This was to clearly see the difference between the discharges as reducing the friction will cause oscillations in the values even at steady state. A smaller friction value will also cause bigger disparities that on figure 10-3.

For the simulations on this report small control values of 1 cm in length were used to ensure precision but control volumes of 2.5 cm were also tested and gave very similar results.

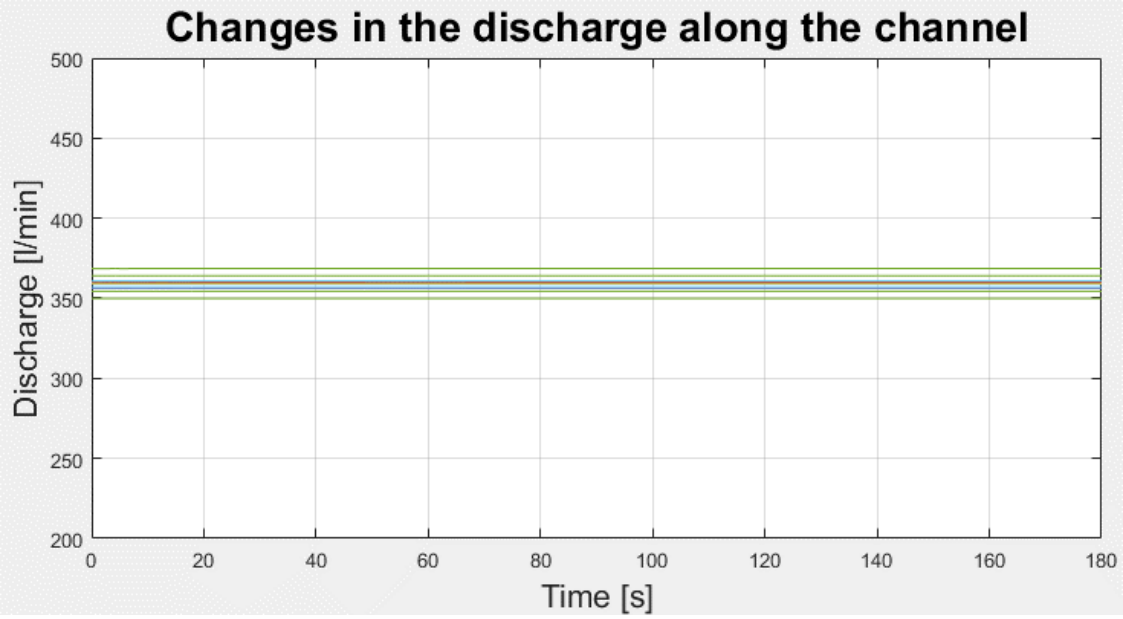

Figure 10-2 Discharges using control volumes with 1 cm in length

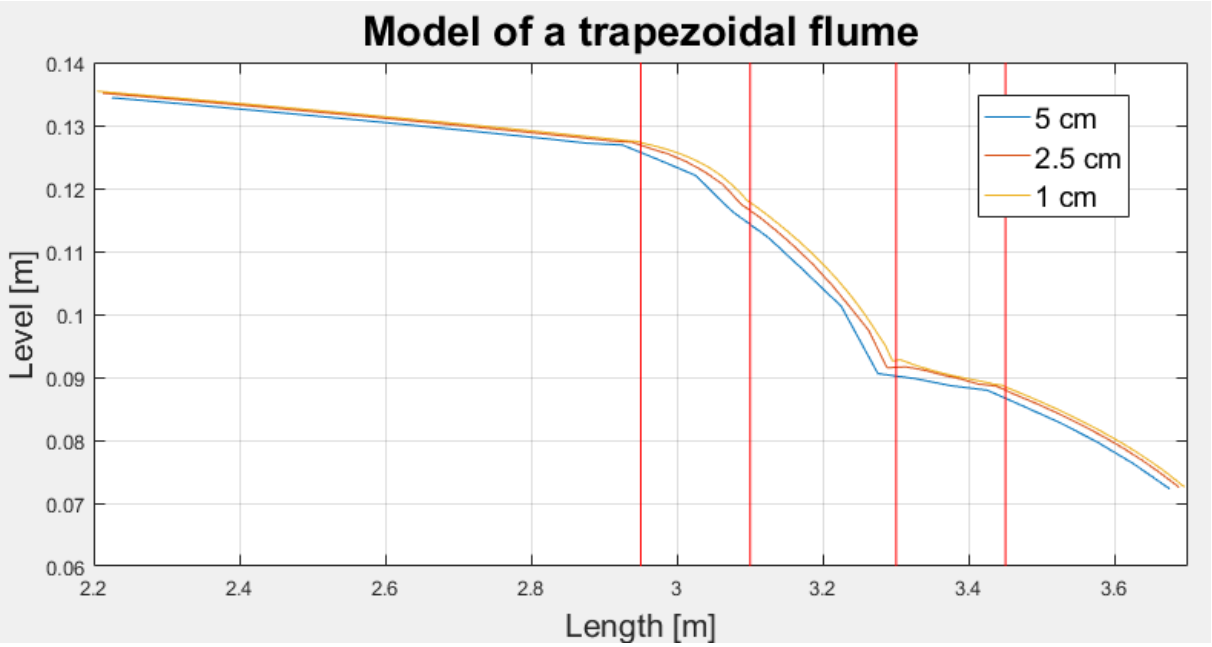

Figure 10-3 Changes in the level with different sizes of control volumes

10.2 Measurements from the Venturi channel

Three ultrasonic meter use to measure the level of flow going through the flume are available and can be placed freely at any point through the channel. The sample time of the sensors is one measurement per second. The discharge is measure using a Coriolis meter for reference. The pump use to push the fluid into the channel is capable to pump from 275 kg/min to around 550 kg/min of fluid.

For the measurements, the sensors were placed as follows: One 160 centimeters from the start, one 235 centimeters from the start near the converging section and the last one at the middle of the throat 305 meters from the start of the channel. A fluid that is a little bit more dense and viscous than water was use during the experiments to simulate real drill mud. The slope of the channel was set to be constant and equal to 0.1 degrees.

The flow discharge from the pump goes into the flume from plastic cylinder. When the fluid level reaches certain level, the fluid falls into the channel as showed in figure 10-4.

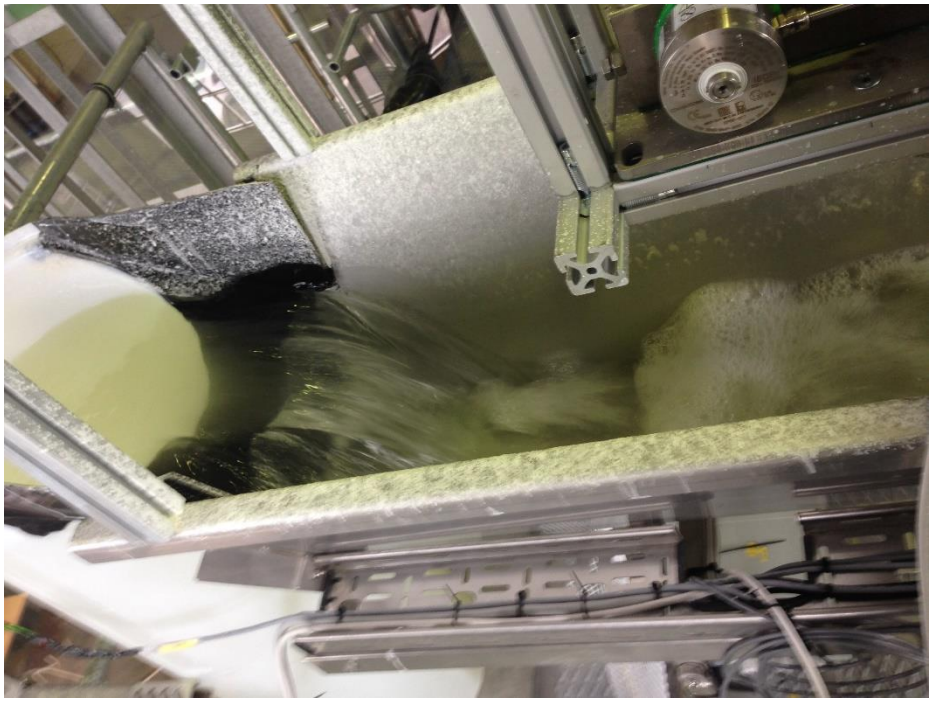

Figure 10-4 Fluid discharge at the start of the Venturi flume

The fluid that falls into the channel will go immediately into supercritical flow, afterwards there will be a hydraulic jump where the flow becomes subcritical. The location of the hydraulic jump along the channel depends on the discharge. A higher discharge means that the hydraulic jump is closer to the start of the channel. This is important to note since after hydraulic jump there will be a lot of waves and turbulence, which will affect the level measurement. This is specially the case while taking measurements with low discharges. There are also bubbles present after the hydraulic jump. Figure 10-5 show these disturbances.

Another disturbance is that the inclination of the flume is not completely stiff and it will move slightly up and down depending on the fluid discharge. These are only presence with

relatively high discharges. The only time when these are visible is when the discharge is larger than 400 kg/min.

In addition to the disturbances, there is also measurement noise from the ultrasonic sensors. A simple moving average filter was used to reduce the effects of noise and disturbances. Multiple sized for the filter were tested. Figure 10-6 shows the raw values and the filtered values using a moving average filter taking the average from 30 measurement, it shows that using this number of samples will get rid of most of the disturbances caused by noise. Note that starting values for the filter were also taken from the experimental data. The values are nerveless still oscillating, this is most likely due to the waves created by the hydraulic jump. Assuming that the changes in the level caused by the waves will have a zero mean, using a larger number of sample will also reduce these disturbances. Figure 10-7 show the results of using a filter that take the averages of 60 measurements, this will compensate for most of the disturbances. Depending on the discharge and the size of the waves, the filter will need up to 180 samples (or three minutes) to successfully neglect the disturbances.

Figure 10-5 Fluid through the Venturi flume

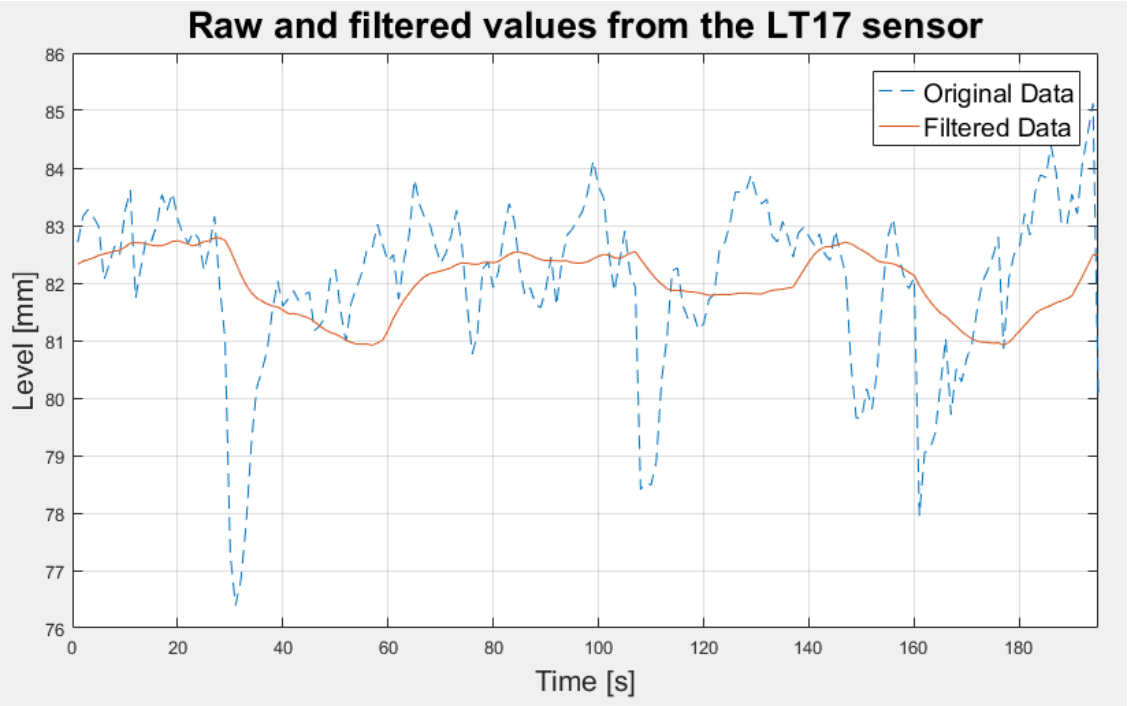

Figure 10-6 Moving average filter using 30 measurements

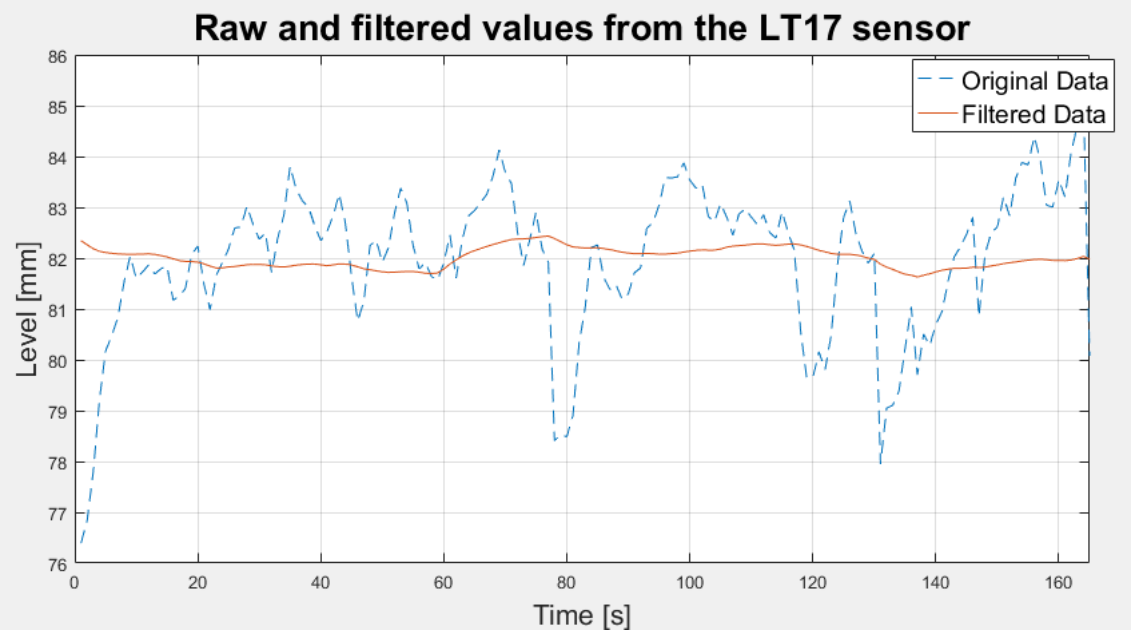

Figure 10-7 Moving average filter using 60 measurements

Several measurements were taken to see the changes in the level with different discharges. For each measurement, the discharge was increased with 20 kg/min each time taking two sets of around 200 samples after the flow went to steady state. Figure 10-8 shows a plot of the mean of these measurements. For reference the first sensor at the upstream (Upstream 1) is

located 160 cm from the start and the second (Upstream 2) is located farther down near the converging section 235 cm from the start. The one at the throat is located exactly at the middle of the throat. These values are not compensated for the slope as this is very small (0.1 degrees) and can be neglected.

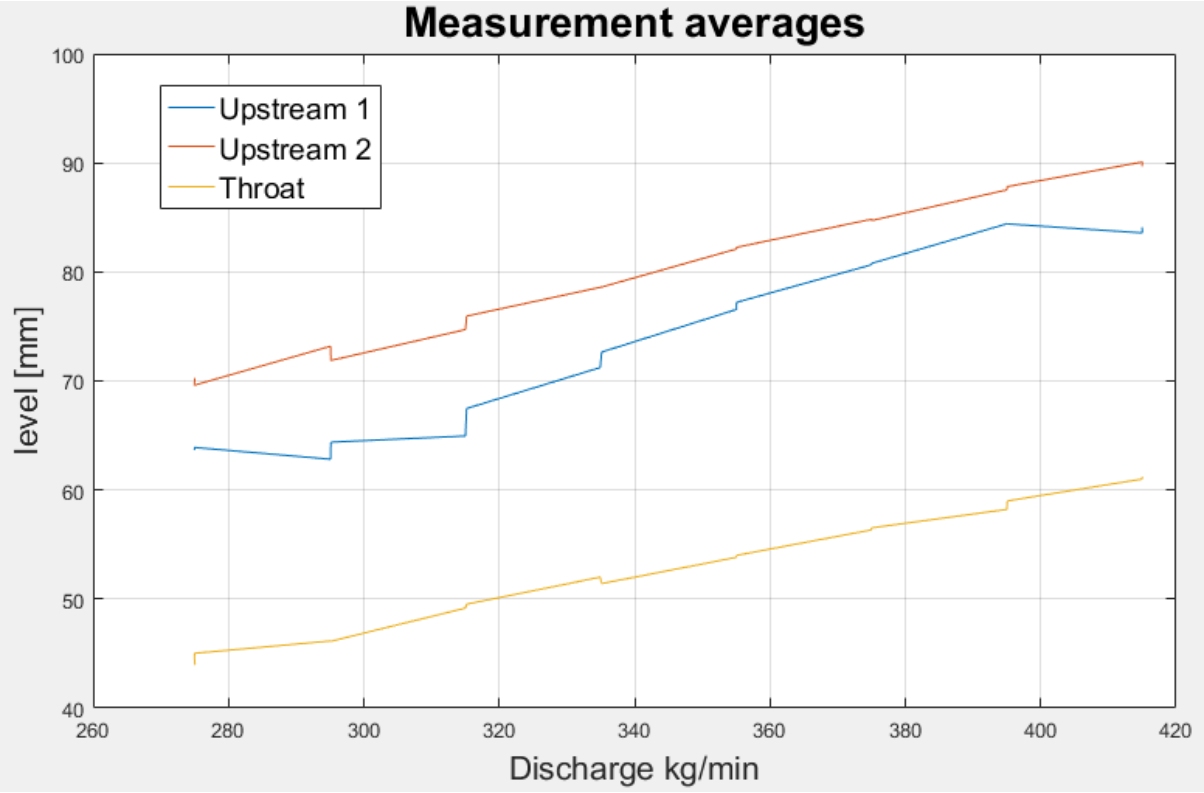

Figure 10-8 Relationship between the flow level and the discharge

10.3 Simulations of the dynamic model of the Venturi flume

Two scenarios were simulated one for a critical depth flume, which means that at some point along the throat the flow is expected to become supercritical, and one for a subcritical depth flume where the flow will always be subcritical. Figure 10-9 shows the flow level along the channel after simulating the model for subcritical flow after reaching steady state. The vertical lines indicate the start and end of the diverging and converging sections of the channel. In contrast figure 10-10 shows the result of simulating for supercritical flow. The small rise in the level prior to the converging section in both simulations is due to the slope of the channel equal to 0.1 degrees.

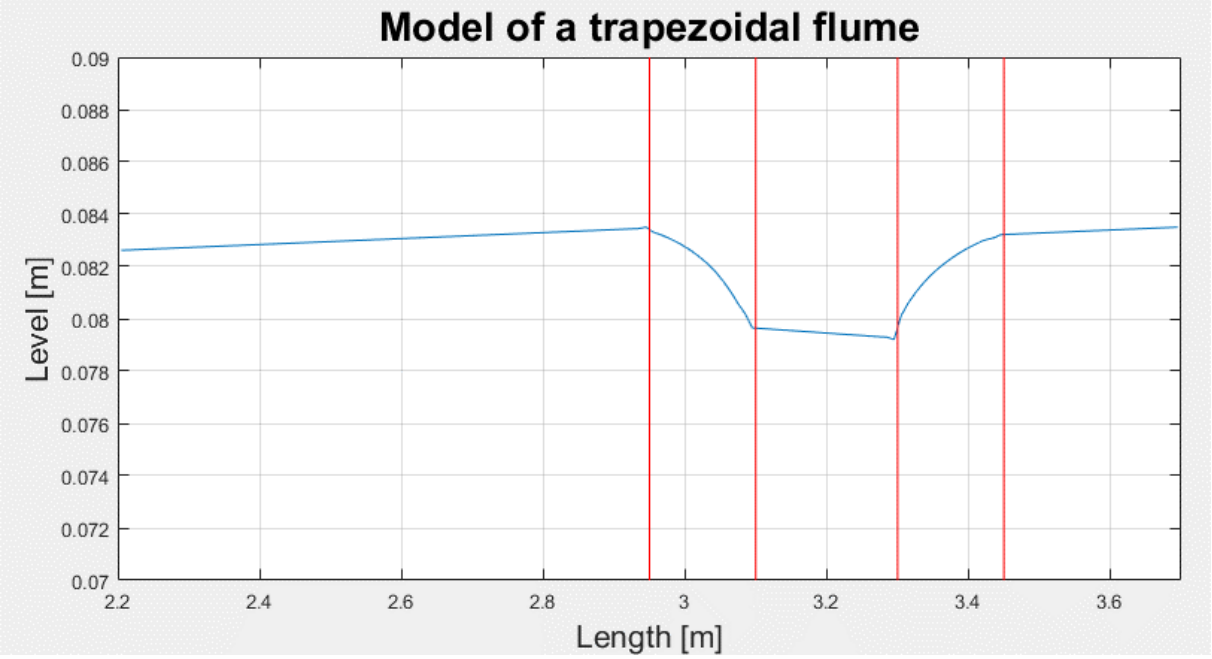

Figure 10-9 Simulation of the model for subcritical depth

Both scenarios were simulated using a low manning's roughness coefficient equal to 0.02. After multiple simulations, this was the value that gave the results that resemble best the values gotten from the measurements.

Figure 8-8 shows how the level decreases when the flow enters the converging section of the channel. In this case, the discharge is not high enough for the level to go down to the critical depth and therefore rises back when passing the diverging section.

In figure 8-9, the discharge is high enough so the flow level goes down the critical depth and the continues to decrease while the water passes through the diverging section of the flume. At the end of this plot is also possible to see a wave that starts being form. This is the start of a hydraulic jump were the flow goes back to subcritical flow.

Here both scenarios were simulated using two boundary condition for the discharge at the start and at the end of the channel i.e. boundaries for subcritical flow.

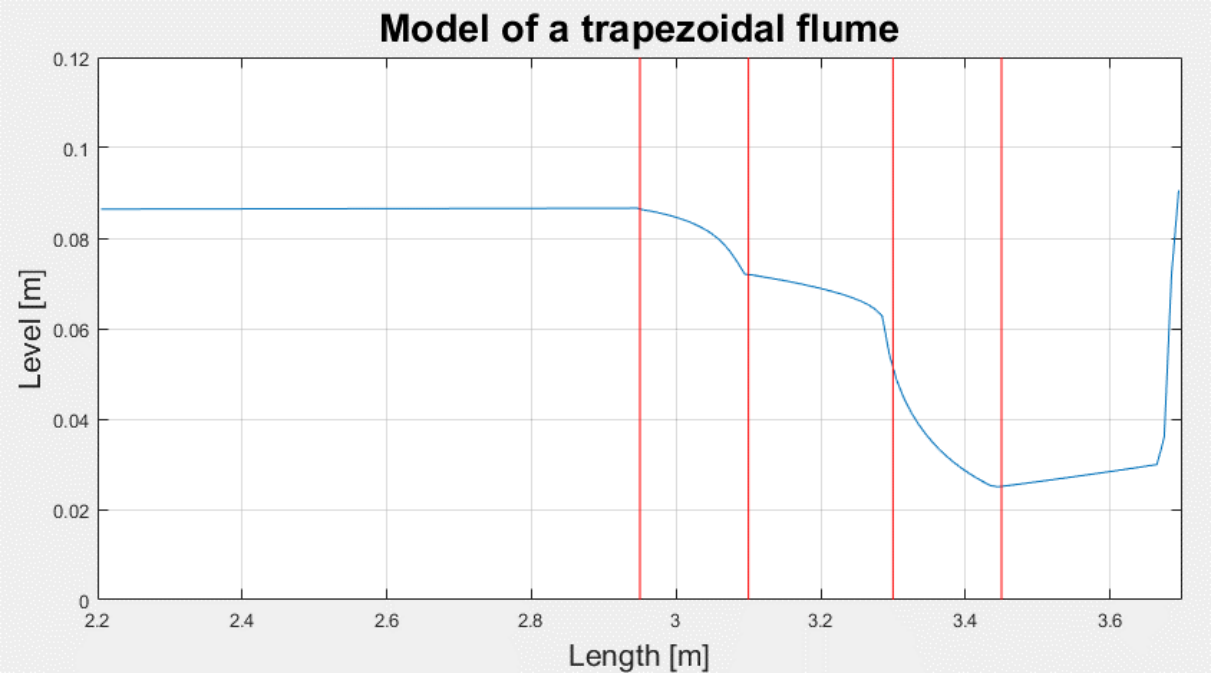

Figure 10-10 Simulation of the model for supercritical depth

One interesting aspect of the KP scheme that emerge during the simulations was the model could converge by using only one boundary condition for the cross-sectional area if the flow was supercritical at the last control volume.

Figure 10-11 shows the results of simulating the channel for supercritical flow, only for the upstream, the converging and the throat and with only one boundary condition at the start for the cross-sectional area. In this example, the level of the initial cross-sectional are is equal to 82 mm.

Using the average of the discharge at the upstream section of the flume and simulating the model again with two boundary conditions will give almost the same result. The initial cross-sectional are was kept the same at 82mm and the discharge gotten from the previous simulation using one boundary condition was 300.62 liters per minute. The comparison is showed in figure 10-12 and the difference are imperceptible.

The model will still converge with one boundary condition when this condition changes during the simulation. This will be demonstrated on chapter 11.

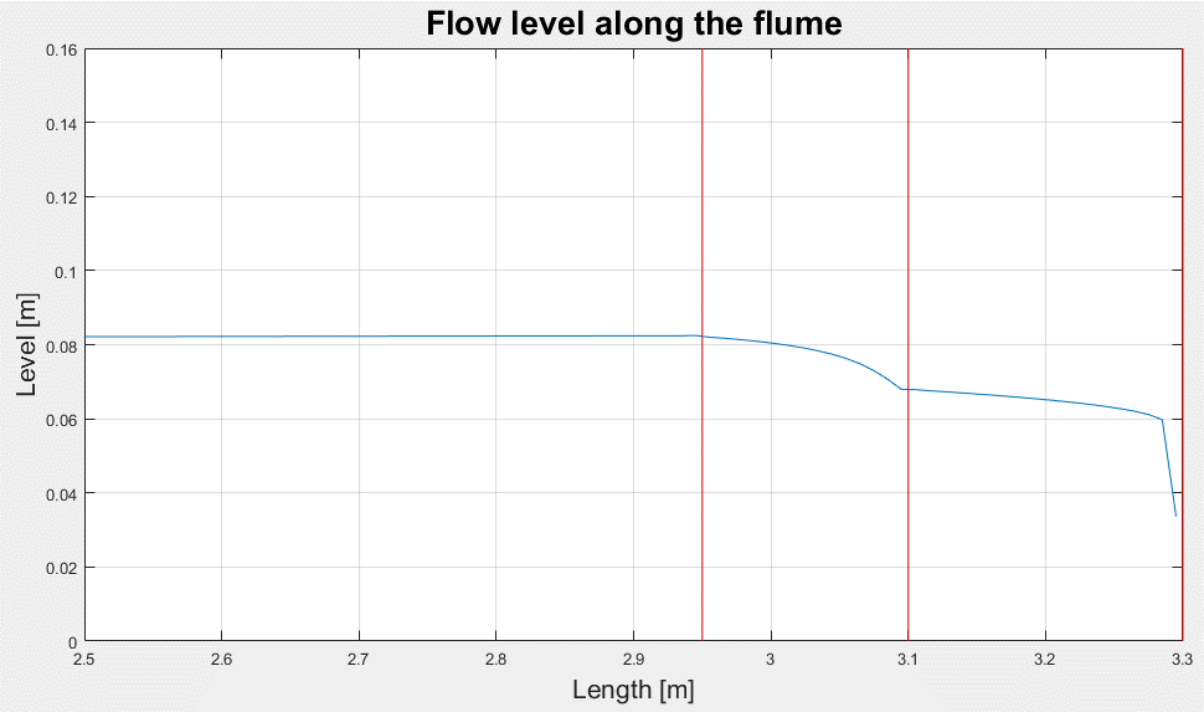

Figure 10-11 Simulation with one boundary condition

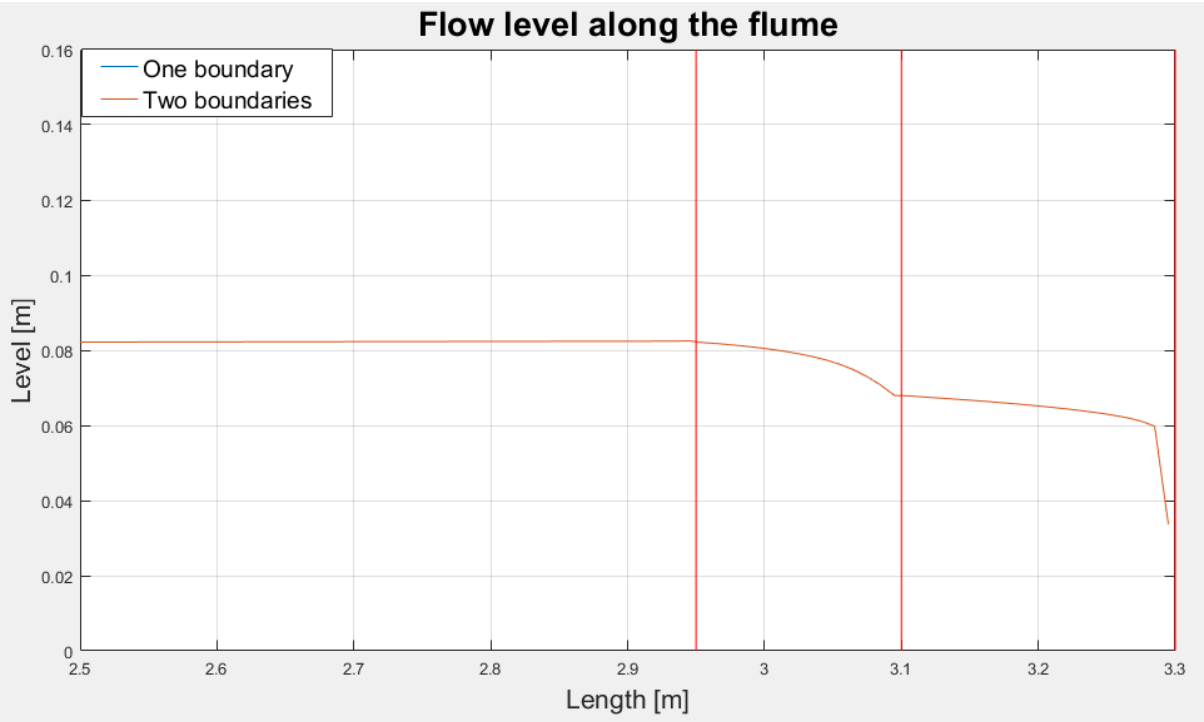

Figure 10-12 Comparison between the results of using one a two boundary conditions

11 Comparing the results of the estimation

There were two methods use to estimate the discharges:

- Using equation 1.10 on chapter 1.2 derived from the Bernoulli's equation with the values from two level sensors, one at the upstream section and one at the middle of the throat.
- Using the dynamic model of the trapezoidal flume with a cross-sectional area calculated using one of the lever sensors located the upstream section. Then using Bernoulli's for the simulated level at the throat. This is partially to see how the simulation works with only one boundary condition.

The discharge estimation using the mean of 16 sets of measurements of around 200 samples each for 8 different discharges (two sets for each) is showed in figure 11-1 using the value from the Coriolis meter as reference.

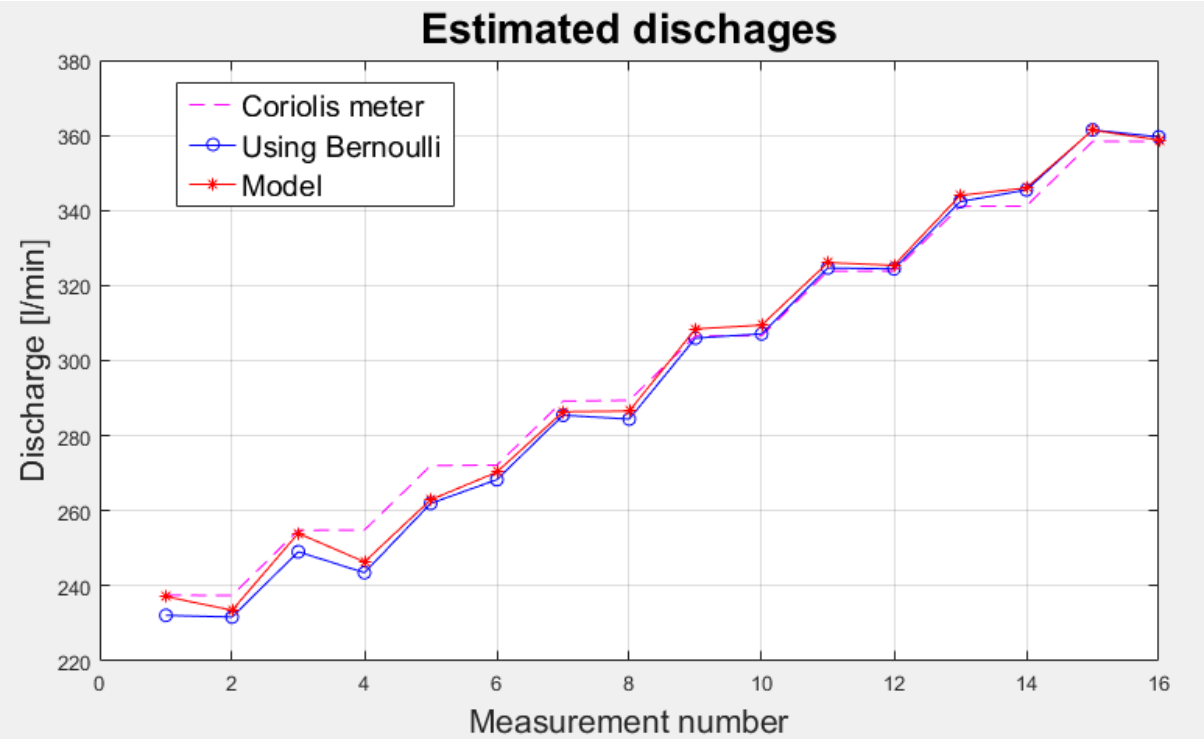

Figure 11-1 Estimation for different discharges

Multiple simulations show a near accurate of the discharge for this fluid. The estimation is more accurate while measuring larger discharges around 300 liters per minute.

Different sizes for the moving average filter were also tested. Figure 11-2 shows the estimation using a 60-sample filter (one sample per second) and figure 11-3 the result of using a 180-sample filter. It shows that the disturbances caused by the wave can be neglected by using a large filter. However, this comes with a large delay as the downside. The delay is showed in figure 11-4. In contrast figure 11-5 show the delay of using 60-sample filter. As

the change in the discharge from the choke valve should not be this abrupt, may still be advisable to use a large group of samples. One comment about figure 11-5 is that at the end of the simulating the sudden change in the discharge is causing some disparities between the estimated and real values, these will go away when the system goes to steady state. For reference this is the same discharge use for figures 11-2 and 11-3.

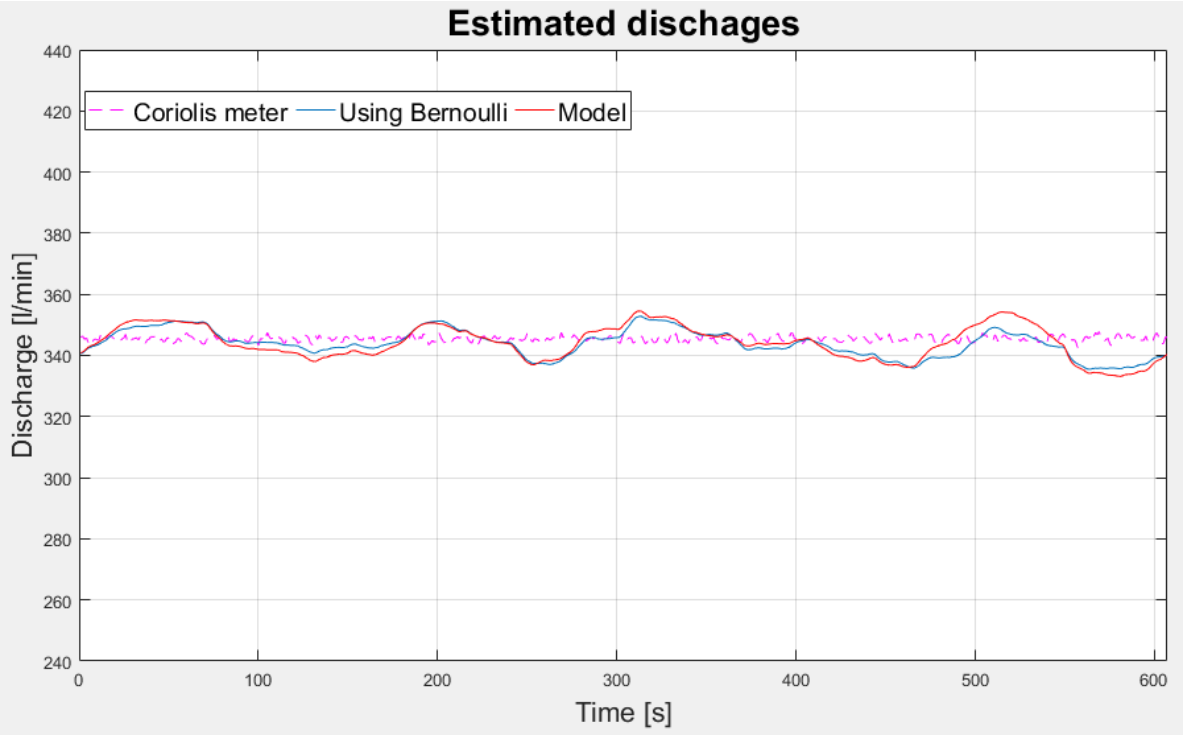

Figure 11-2 Estimation using a 60-sample moving average filter

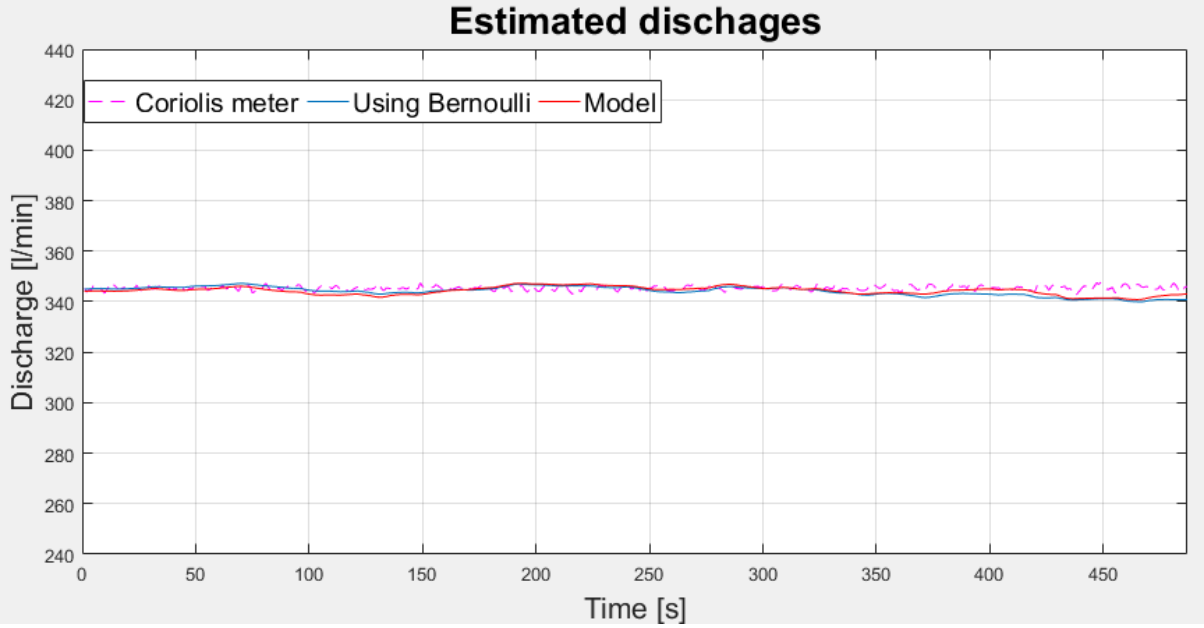

Figure 11-3 Estimation using a 180-sample moving average filter

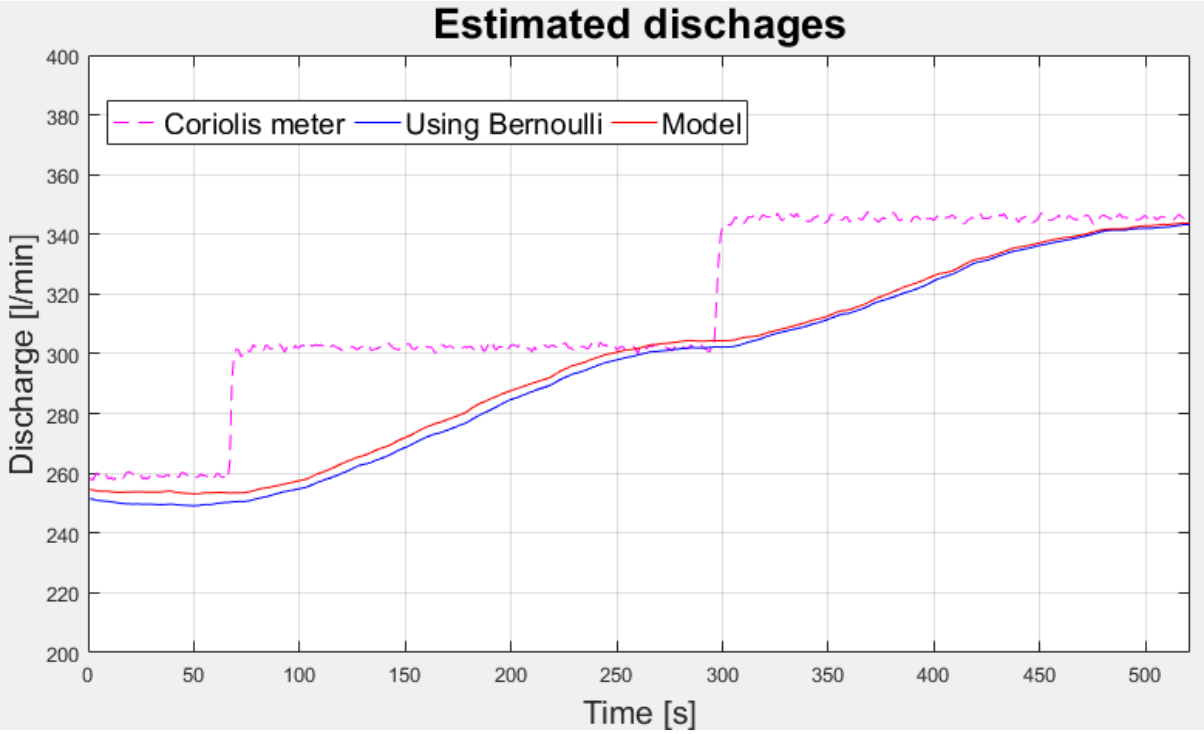

Figure 11-4 Delay from a 180-sample moving average filter

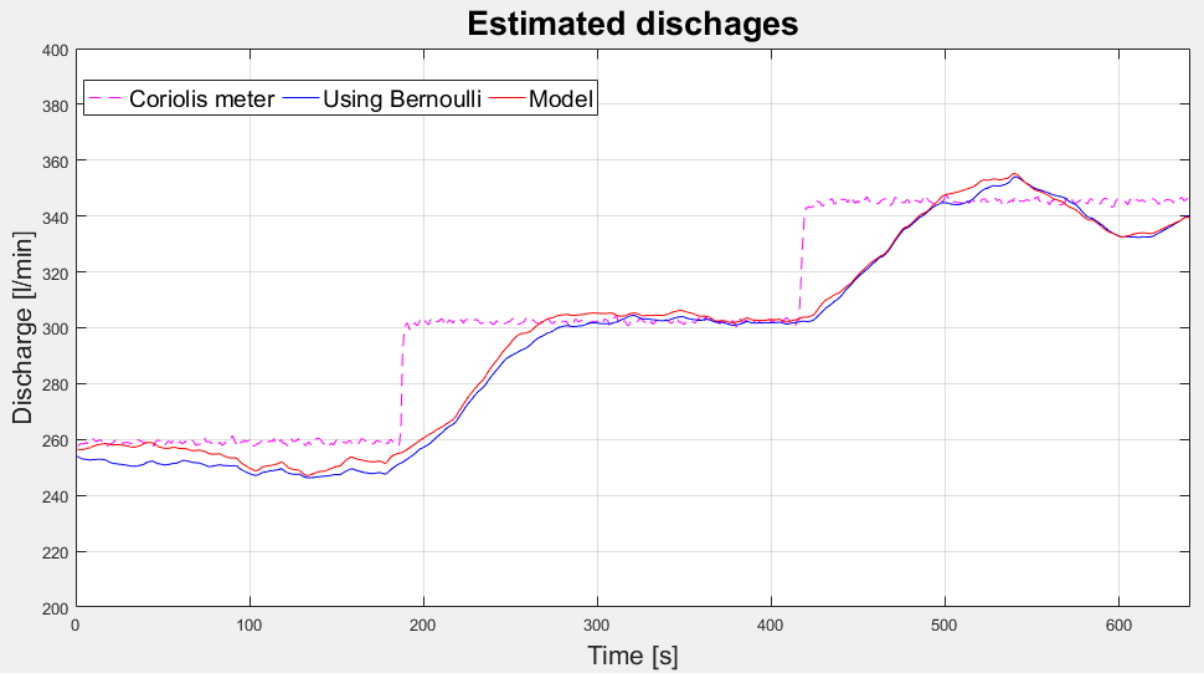

Figure 11-5 Delay for a 60-sample moving average filter

As showed in figure 11-1, the estimation is worse for small discharges. Another set of values with a smaller step change was used to test the estimation and results are showed in figure 11-6 for 180 samples and figure 11-7 for 60 samples.

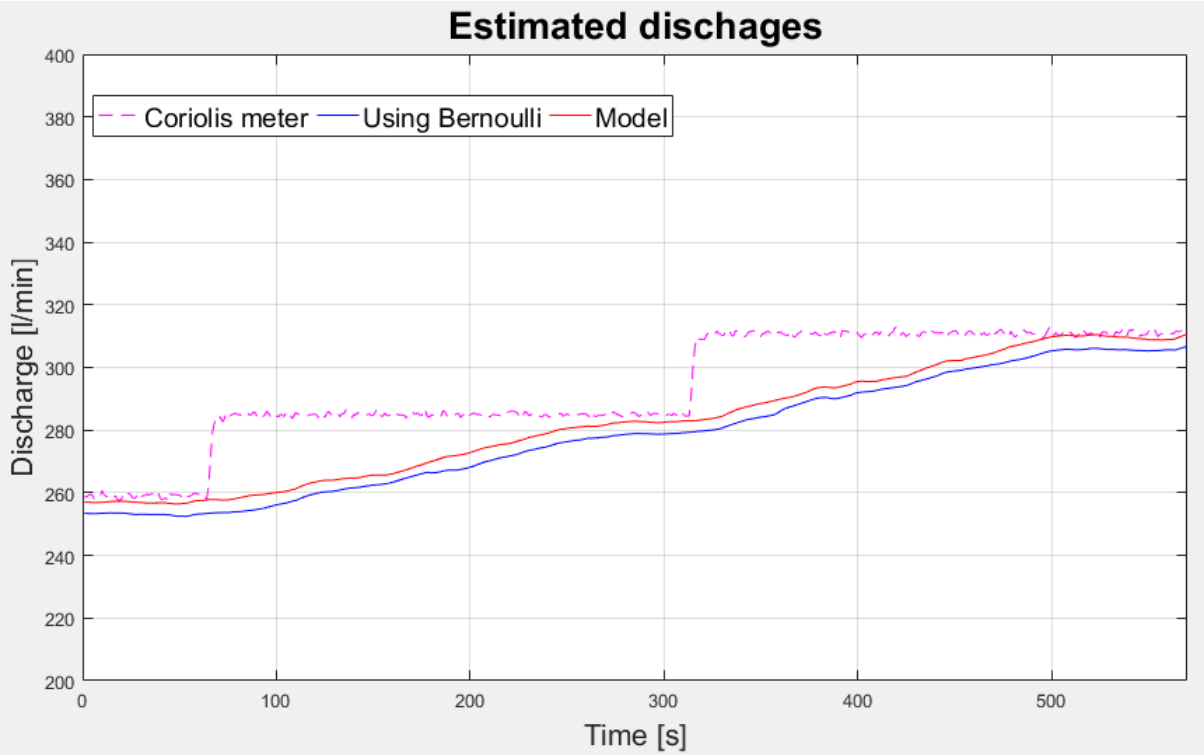

Figure 11-6 Delay from a 180-sample moving average filter second set

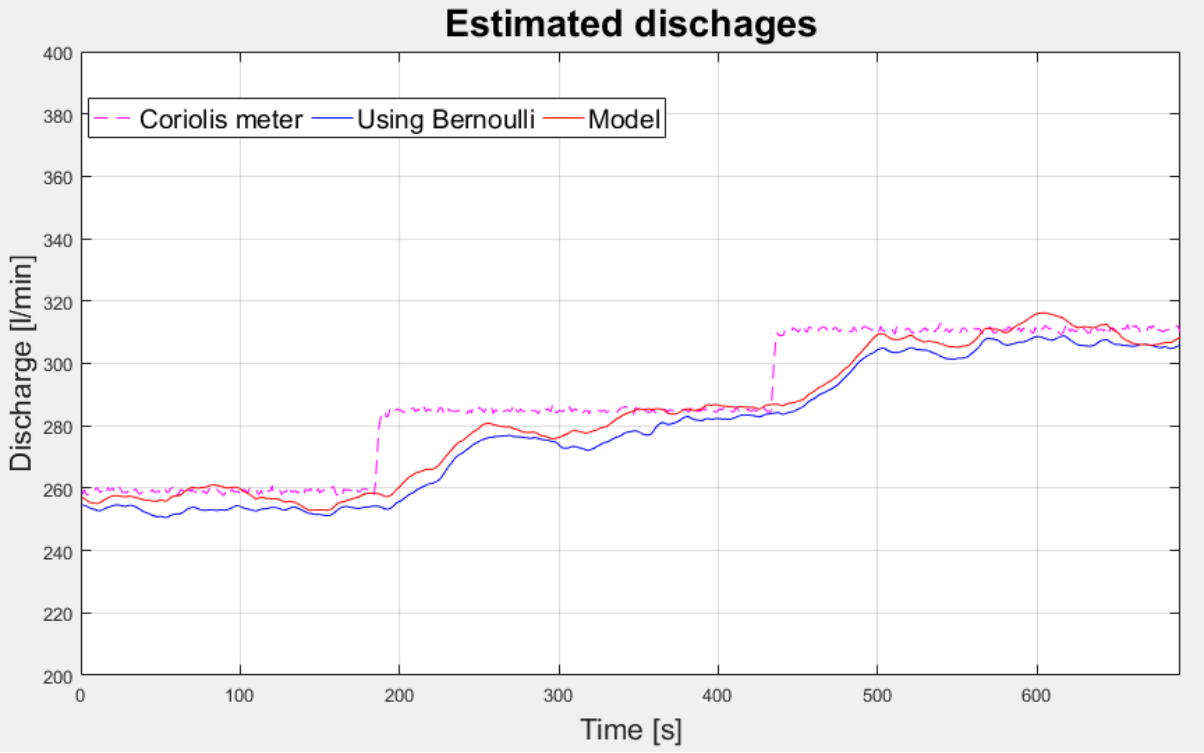

Figure 11-7 Delay for a 60-sample moving average filter second set

The results still close to the real values specially for the large filter.

One more value of interest is the value for the discharge from the simulation as it goes unbounded. This value has a lager error that the other two values but still close to the real value as showed in figure 11-8. This discharge was taken as the average discharge of the cells at the upstream section of the flume.

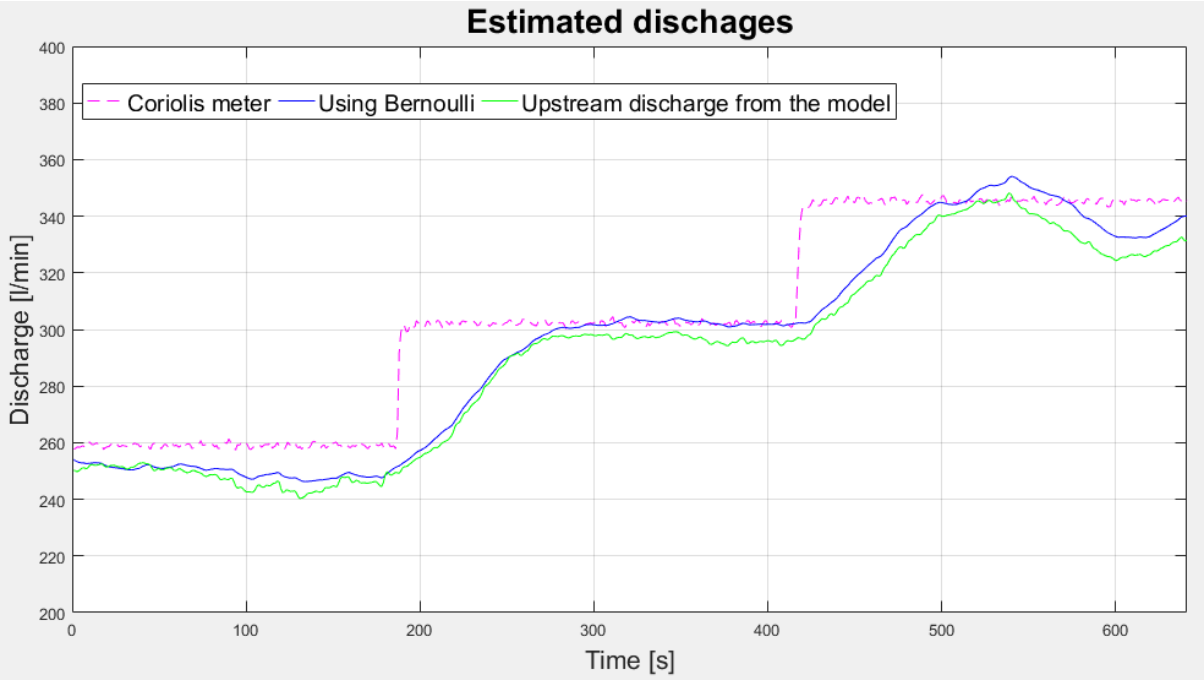

Figure 11-8 Simulated discharges using only one boundary condition

Is possible that with a good value for the friction, this value will always give a good estimation for the discharge even with large friction values where the error from the Bernoulli's may be too big.

Part III

Conclusions and future works

12 Future works

12.1 For the top flow model

The model has not been validated and there are some important that need to be answer with the help of experimental data.

- As the model currently neglects the delay done through the solid control system, it is important to know how big is this delay. The solid control system with equipment, pump, changes in the density and viscosity and the fact that it has no standard is too complex to create a model of. In case that the delay is too big to be neglected, a delay model based on measurements may be the best alternative.
- There needs to be a suitable estimator for the loses of drill mud through the solid control system. This can be based on the rate of penetration, common values for the fluid retention of solids and the efficiency of the solid control system. Taking in consideration the possible sudden enlargement of the annulus (washout).
- Study the delay of the system and discuss the possibility of using the model for early kick detection with the level measurements of the mud pits. It is also possible to use the level measurement of the first partition of the mud pit after the degasser instead of the level at the active pit. This is in the case the delay through the solid control system is too big and the fluid losses due to the rest of the equipment (e.g. mud cleaner, decanting centrifuge) can be neglected.

Also, the need of a level sensor at the start of the flowline should be discuss. It is possible that the result using only the discharge as the boundary condition can give satisfactory results.

12.2 For the flow estimator

The estimator was only tested with one type of fluid. As the fluid coming though the return line will include cuttings, it is important to test the estimation with more viscous fluids.

As mention on chapter 10.2 since the slope of the channel when taking the measurements was very low, the value was not adjusted. This was partially because the angle changed a lot with large discharges. It still may be important to compensate for this value as small changes of just a couple of millimeters can change the result of the estimation. It could possible that the value from the upstream cells in the model was closer to the real value that the value from using the Bernoulli's equation.

The error that appears while estimating the discharge for low discharges is possible that is due to the friction. A better solution may be to have an adaptable friction term in the model.

Lastly the model uses manning's equation to model the friction, as drill mud is non-Newtonian it can be modeled using the Herscher-Bulkley model if the results are not satisfactory.

13 Conclusion

13.1 Concluding remarks for the model of the top flow loop

The idea behind the project was to create a model for the top flow loop of a drilling operation. This model could then use small changes in the level of the mud pit to estimate the occurrence of a kick or other irregularities.

A simple model for the circulation of drilling mud through return line and into the mud pits during a drilling operation was developed. The flowline was modeled using the Saint Venant equations which were solved using the second order central upwind scheme. The mud pit was modeled using some simple calculation for the mass balance. A model of the solid control system would be too complex to be made. Alternatively, the model can use an estimator to compensate for the losses of drill mud through the system. The delay though the solid control system can either be neglected or modelled using experimental data.

The model was then combine with another model for the circulation of drill mud in and out of a drilling well and simulated for three operational scenarios: during surge and swab, for a pipe connection procedure and during a sudden influx of fluid from the reservoir. The results are seemly correct although the model has not been validated.

13.2 Concluding remarks for the flow estimator

An alternative way to measure the discharge of drill fluid from the return line is by using a Venturi channel in combination with ultrasonic sensors to measure the flow level. Flow estimation through this type of channels is done normally by using the Bernoulli's equation with the downside that the equation ignores friction.

A model of the Venturi was develop using the Saint Venant equations which were solved using the second order central upwind scheme. After several simulations, it was found out that the model seems to converge by using only one boundary condition at the start for the cross-sectional area of the flow without a boundary condition for the discharge when running the model for supercritical flow.

Several measurements were taken from a real Venturi to validate the model and compare the results from the estimation using Bernoulli's equation. The results were similar as the viscosity of the fluid use for the measurements was not high enough for the Bernoulli's equation to show a considerable error.

More experiments using a fluid that better resembles the flow thought the Venturi channel is recommended to study if the friction would cause the error of the Bernoulli's to become too large, and if that is the case if the model of the Venturi channel can still give good predictions regardless of the friction.

References

1. *Drilling fluids and health risk management*. 2009, IPIECA, OGP: London, United Kingdom.
2. Kaasa, G.O., *A simple dynamic model of drilling for control*. 2007: Porsgrunn.
3. Stamnes, Ø.N., *Adaptive oObserver for bottomhole pressure drilling*, in *Departament of Engineering Cybernetics*. 2007, Norwegian University of science and Technology.
4. Grace, R.D., *Advanced Blowout & Well Control*. 1994, Houston, Texas: Gulf Publishing Company.
5. *Drilling Fluids reference manual*, in *Baker Hughes*. 2006.
6. Adam T. Bourgoyne Jr, K.K.M., Martin E. Chevevert, F.S. Young Jr., *Applied Drilling Engineering*. SPE, ed. D.S.P. Jack F. Evers. 1986: Society of Petroleum Engineers.
7. Growcock, F. and T. Harvey, *Chapter 2 - Drilling Fluids*, in *Drilling Fluids Processing Handbook*. 2005, Gulf Professional Publishing: Burlington. p. 15-68.
8. Robinson, L., *Chapter 15 - Dilution*, in *Drilling Fluids Processing Handbook*. 2005, Gulf Professional Publishing: Burlington. p. 335-366.
9. American Association of Drilling, E., *Chapter Two - The Role of Shale Shakers*, in *Shale Shaker and Drilling Fluids Systems*. 1999, Gulf Professional Publishing: Burlington. p. 91-96.
10. American Association of Drilling, E., *Chapter Six - Shale Shaker Screens*, in *Shale Shaker and Drilling Fluids Systems*. 1999, Gulf Professional Publishing: Burlington. p. 120-138.
11. *Working principle of shale shakers* [cited 2017 May 1]; Available from: http://www.weiku.com/products/5744951/JZS180_2P_drilling_fluid_shale_shaker.html.
12. Morgan, M.C., *Chapter 6 - Scalping Shakers and Gumbo Removal*, in *Drilling Fluids Processing Handbook*. 2005, Gulf Professional Publishing: Burlington. p. 107-110.
13. Morgan, M.C., *Chapter 11 - Hydrocyclones*, in *Drilling Fluids Processing Handbook*. 2005, Gulf Professional Publishing: Burlington. p. 257-282.
14. *Operating Principle of Hydrocyclone*. [cited 2017 May 1]; Available from: http://www.gn-shale-shaker.com/operating-principle-of-hydrocyclone/.
15. Bouse, E., *Chapter 13 - Centrifuges*, in *Drilling Fluids Processing Handbook*. 2005, Gulf Professional Publishing: Burlington. p. 303-326.
16. *TYPICAL DETAILS OF CENTRIFUGE*. 2001 [cited 2017 May 1]; Available from: https://law.resource.org/pub/in/bis/S03/is.10037.3.1983.html.
17. Morgan, M.C., *Chapter 5 - Tank Arrangement*, in *Drilling Fluids Processing Handbook*. 2005, Gulf Professional Publishing: Burlington. p. 93-106.
18. *Solids control Handbook*. 2009, NOV.
19. Robinson, L., *Chapter 8 - Settling Pits*, in *Drilling Fluids Processing Handbook*. 2005, Gulf Professional Publishing: Burlington. p. 183-188.
20. *Solids Control and Recycling*. [cited 2017 May 1]; Available from: http://www.ptarmiganservices.com/news/bakken-solids-control-and-recycling/.

21. Carey A. Johnston, M.R., *Development Document for Final Effluent Limitations Guidelines and Standards for Synthetic-Based Drilling Fluids and other Non-Aqueous Drilling Fluids in the Oil and Gas Extraction Point Source Category*, E.P. Agency, Editor. 2000, EPA: Washington, DC.
22. *Compact MD-2 Shaker Outperforms Competition in Eagle Ford Shale Test for Cheyenne Petroleum*. 2015 [cited 2015 May 1]; Available from: http://www.slb.com/resources/case_studies/miswaco/md2_eagle_ford.aspx.
23. Sleigh, A., *Fluid Mechanics*. 2000, University of Leeds.
24. *Offshore and Onshore Pipeline Solutions*. 2010 [cited 2017 May 1]; Available from: www.tenaris.com.
25. Arturo S. Leon, M.S.G., Arthur R. Schmidt, Marcelo H. Garcia, *Godunov-Type Solutions For Transient Flows In Sewers.* Journal of Hydraulic Engineering, 2005. **132**(8).
26. Sharma, R., *Second order scheme for open channel flow*. 2015, University college of South-East Norway Porsgrunn, Norway.
27. Hickin, E.J., *River Hydraulics and Channel Form*. 1996: Simon Fraser University.
28. Cairns, M.M., *Meteorology glossary*. 2014: American Meteorological Society.
29. Robinson, A.R., *Trapezoidal Flumes For Measuring Flow In Irrigation Channels*. 1968, UNITED STATES DEPARTMENT OF AGRICULTURE.
30. Sleigh, D.A., *An Introduction to Fluid Mechanics*. 2001, University of Leeds.

Appendices

List of appendices:

- Appendix A: Description of the project
- Appendix B: Calculations for flow through circular pipes
- Appendix C: Calculations for flow through trapezoidal pipes
- Appendix D: Matlab Codes

Appendix A

Description of the project

<Next page>

University College of Southeast Norway

Faculty of Technology, Natural Sciences and Maritime Sciences, Campus Porsgrunn

FMH606 Master's Thesis

Title: **Modelling and estimation for return mud flow during drilling**

HSN supervisor: Roshan Sharma, Asso. Prof., University College of Southeast Norway

External partner: Statoil, Kelda drilling controls ASA

Task background:
Foreword: This master thesis is a part of the on-going "Semi-Kidd" project at USN (which involves 4 PhD students working with the project) financed by Statoil and Norwegian Research Council.

During drilling, drill fluid is injected into the well being drilled using mud pump as shown in Figure 1. This drill fluid will carry away the drill cuttings from the bottom of the well and transport them back to the top through the return line.

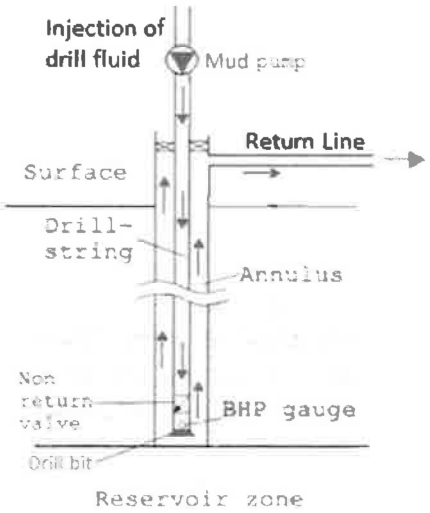

Figure 1: Schematic of fluid flow in drilling

On the top side, the drill fluid is cleaned and re-injected into the well. Accurate and real time measurement of the flow of drill fluid in the return line is vital for a safe operation. Coriolis flow meters which are used in practice are very expensive and unreliable. So, in this thesis, we focus on answering the following questions:
Can we instead use a suitable mathematical model of the fluid flow to estimate the mud flow in the return line?
Can we replace the expensive sensor with model based measurement/estimation?

During drilling, the pressure at the bottom of the well (BHP) should be tightly regulated. If this pressure is too much, then it will fracture the well and the drill fluid will be lost into the formation (reservoir zone). If this pressure is too little, then formation (reservoir) fluid may enter into the well (in annulus) during drilling. This is known as kick. If the occurrence of a kick is not regulated, then uncontrolled flow of reservoir fluid into the well and then out to

Address: Kjølnes ring 56, NO-3918 Porsgrunn, Norway. **Phone:** 35 57 50 00. **Fax:** 35 55 75 47.

the surface may occur. This is known as blow out of the well and is disastrous and highly unwanted situation.
The knowledge of how much drill fluid is flowing in the return line can provide an early warning about a kick or a loss. If the flow in the return line is more than what is injected into the well, probably some fluid from the reservoir have entered into the well i.e. a kick might have occurred. Conversely, if the flow in the return line is less than what is injected into the well, probably some of the fluid fluid from the well have leaked into the reservoir zone. Thus, flow rate of the fluid in the return line is a primary indicator of a kick or a loss.

In University College of Southeast Norway, a venturi channel (which is an open channel) rig has been constructed to measure the flow rate of the return drill fluid. The idea is to place the venturi channel in the return line to estimate the return fluid flow. Such venturi channels are also used in irrigation canals (and/or smaller rivers) to measure the flow rate.

The work is open to all the students from IIA, PT and EET.

Task description:
Development of a mathematical model for return flow line for estimation of flow is the main task.

1. Give an overview of the drilling process and explain the importance of early kick/loss detection.
2. Perform a thorough literature survey about the drain back to the active mud pit that makes up the closed loop drill mud circulating system.
3. Develop a simple model of the drain back to the active pit for the top side flowline. Combine the top side model with the bottom side drilling model. Simulate the combined model for various operational scenarios.
4. Explain in detail the different terms involved in 1D shallow water equations (Saint Venant equations). Simulate the Saint Venant equations using the Kurganov Petrova scheme for flows through the venturi rig.
5. For model validation, carefully planned experiments should be performed on the venturi rig (in the process hall) for obtaining experimental data. These data should be used to validate the model and to calculate the unknown model parameters.
6. By making use of the fluid level measured by the ultrasonic sensors, estimate the flowrate through the venturi channel using a suitable estimator.
7. Report the work in the Master's Thesis. Present the thesis work.

Student category: Open for all students from PT, IIA and EET

Practical arrangements:
Perform experiments in the venturi rig at USN.

Signatures:

Student (date and signature):
16.01.2017
Supervisor (date and signature):
16.01.2017

Appendix B

Calculations for flow through circular pipes

This appendix explains in detail the equations to calculate the cross-sectional area, the level and the wetter perimeter of flow through circular pipes.

The cross-sectional area of the flow can be considered as a segment of a circle.

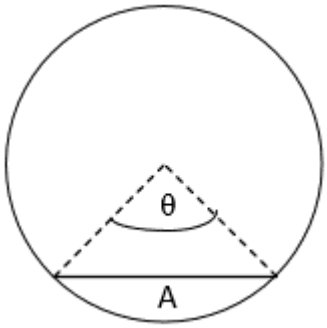

Figure 1 Segment of a circle

The cross-sectional area of the flow inside the pipe will be equal to the area of the section of the circle minus the area of the triangle enclosed by the secant and two radii showed in figure 1. This can be calculated as a function of the angle between the radii and the diameter.

$$Area\ of\ the\ triangle: a_{tri} = \frac{1}{8} r^2 \sin(\theta) \quad (1)$$

$$Area\ of\ the\ section: a_{sec} = \left(\frac{\theta}{2\pi}\right) \pi \frac{D^2}{4} = \frac{\theta}{8} D^2 \quad (2)$$

$$Area\ of\ the\ segment: a_{seg} = a_{sec} - a_{tri}$$

The formula for the cross-sectional area of the flow:

$$A = \frac{1}{8} D^2 (\theta - \sin(\theta)) \quad (3)$$

The level of the flow is equal to the height of the arc also called sagitta. This is equal to the radius minus the height of the triangle in figure 1. The formula is as follows:

$$h = \frac{D}{2}\left(1 - \cos\left(\frac{\theta}{2}\right)\right) \quad (4)$$

The wetted perimeter is equal to the length of the arc.

$$P_w = \left(\frac{\theta}{2\pi}\right) \pi D = \frac{\theta D}{2} = D \arccos\left(\frac{D - 2h}{D}\right) \quad (5)$$

The length of the free surface is equal to the length of the secant.

$$T = D \sin\left(\frac{\theta}{2}\right) \quad (6)$$

Combining equations (4) and (6) will give the formula for the free surface as a formula of the level:

$$T = 2\sqrt{hD - h^2} \quad (7)$$

It is not possible to calculate the height of the flow directly as a function of the cross-sectional area. This can be approximate with the use of the secant method to find the angle θ (equation 3) and then use it to calculate the level. Newton's method is not recommended as it can cause division by zero. Alternative to avoid the use of theta, one can combine equations (3) and (4).

$$A = \left(\frac{D}{2}\right)^2 \arccos\left(\frac{D-2h}{D}\right) - \left(\frac{D}{2} - h\right)\sqrt{h(D-h)} \quad (8)$$

Appendix C

Calculations for flow through trapezoidal pipes

This appendix shows the equations to calculate the cross-sectional area, the level and the wetted perimeter of flow through trapezoidal channels.

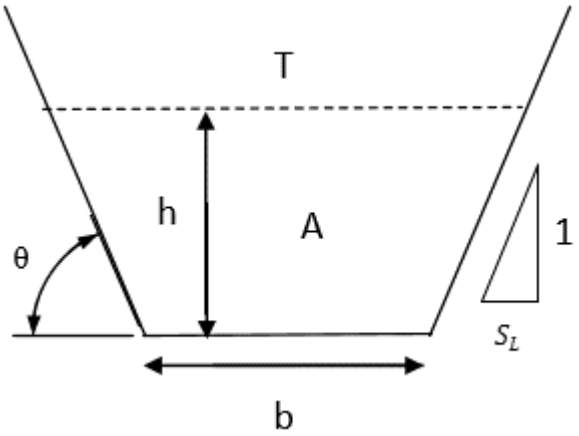

The side slope is the change in the width for each unit of height.

$$S_L = \frac{1}{\tan(\theta)} \quad (1)$$

The cross-sectional are of the flow is equal to the base with times the level plus the area of the triangle created by the side slope. The formula for the cross-sectional area of the flow is the following:

$$A = (S_L h + b)h \quad (2)$$

To get the level as a function of the cross-sectional area a method such as Newton's method or the secant method needs to be implemented.

The wetted perimeter can be formulated as follows:

$$P_w = 2h\sqrt{1 + {S_L}^2} + b \quad (3)$$

The formula for the free surface is the following:

$$T = 2S_L h + b \quad (4)$$

Appendix D

The following codes were summited in a zip file along with a digital copy of the thesis:

- Model of the flowline
- Model of the combine model
- Model of the trapezoidal flume
- Modify model of the trapezoidal flume to be simulated with one boundary condition